Systematic investigation of photon strength functions with monochromatic γ-ray beams

Ioana Gheorghe

for the PHOENIX collaboration

Horia Hulubei National Institute for R&D in Physics and Nuclear Engineering (IFIN-HH)

ioana.gheorghe@nipne.ro

This work was supported by a grant of the Ministry of Research, Innovation and Digitization, CNCS - UEFISCDI, project number PN-III-P1-1.1-PD-2021-0468, within PNCDI III.

July 10 2023

International Atomic Energy Agency
CRP on Photonuclear Data and Photon Strength Functions

Code F41032; Duration 2016-2019 https://www-nds.iaea.org/CRP-photonuclear/

Project Officer: P. Dimitriou

CSIs

T. Belgya (CER / Hungarian Acad. of Sc., Hungary)
Y-S. Cho (KAERI, S. Korea)
D. Filipescu (IFIN-HH, Romania)
R. Firestone (University of California, Berkely, USA)
S. Goriely (Université Libre de Bruxelles, Belgium)
N. Iwamoto (JAEA, Japan)
M. Krticka (Charles University in Prague, Czech Rep.)
V. Plujko (Taras Shevchenko National Univ., Ukraine)
R. Schwengner (HZDR, Germany)
S. Siem (University of Oslo, Norway)
H. Utsunomiya (Konan University, Japan)
V. Varlamov (Moscow State Univ., Russian Federation)
M. Wiedeking (iThemba LABS, S. Africa)
R. Xu (CIAE, China)

Advisors

T. Kawano (LANL, USA)
J. Kopecky (JUKO Research, The Netherlands)
P. Oblozinsky (Slovakia)

Reference Database of Photon Strength Functions
Database containing all the experimental and global theoretical photon strength functions

- Goriely, et al., Eur.Phys.J. A**55**, 172 (2019)

Updated Photonuclear Data Library
IAEA Photonuclear Data Library 2019

- Kawano, et al., Nuclear Data Sheets **163**, 109 (2020)

Long standing discrepancies between Saclay and Livermore data sets

The majority of experimental data for partial photonuclear reaction cross sections were obtained at Livermore (USA) and Saclay (France)
Atlas of Photoneutron cross sections obtained with monoenergetic photons
`S.S.Dietrich, B.L.Berman. Atom. Data and Nucl. Data Tables, 38 (1988) 199`
Bermans library: EXFOR entries L0001 – L0059 ($\sim$ 174 data sets)
Large discrepancies between (γ, xn) cross sections measured at the Saclay and Livermore facilities:

- (γ, n) cross sections generally larger at Saclay than at Livermore
- (γ, $2n$) cross sections generally larger at Livermore than at Saclay

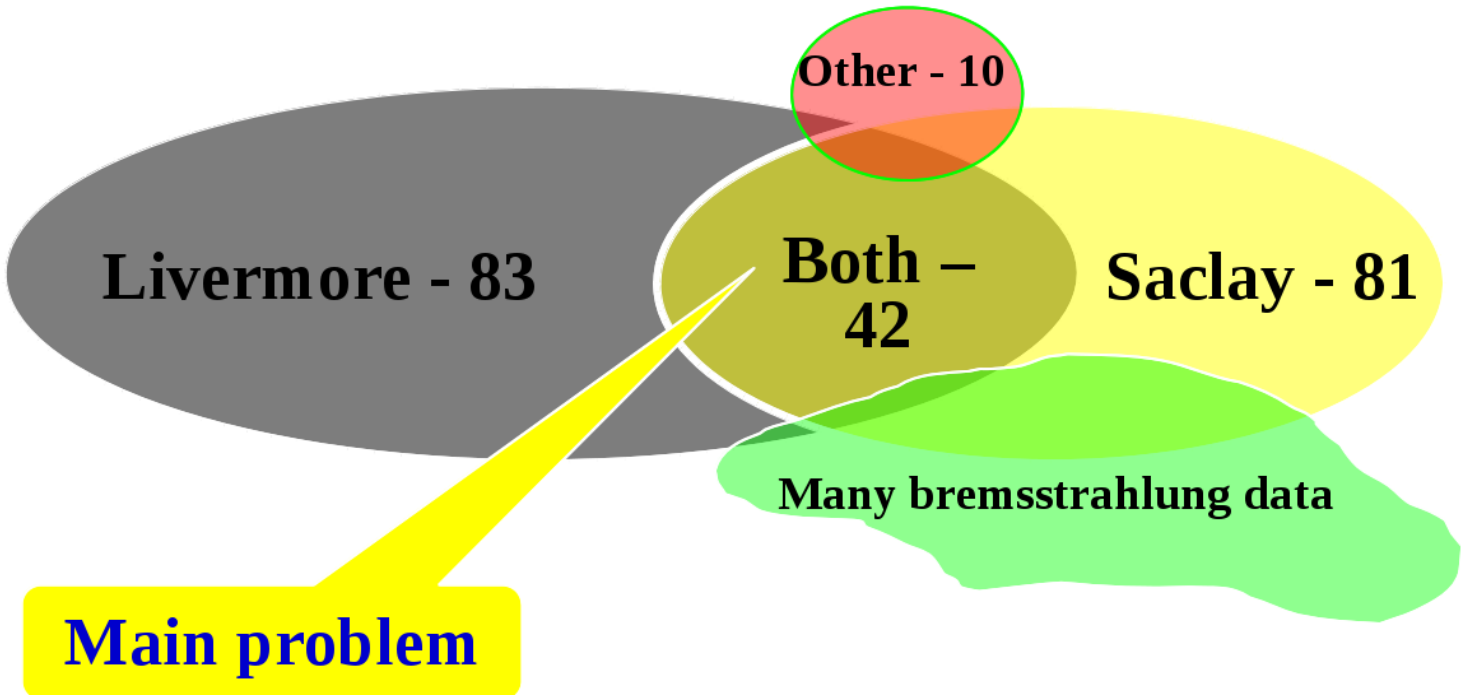

Courtesy of V.Varlamov

NewSUBARU (γ, xn) cross section measurements for IAEA PD CRP

New photoneutron measurements in the Giant Dipole Resonance (GDR):

- quasi-monochromatic Laser Compton scattering (LCS) γ-ray beams
- flat efficiency neutron detector (FED) ▸ H. Utsunomiya, I. Gheorghe, et. al, NIM A 871, 135-141 (2017)

2015	^{209}Bi, ^{9}Be
2016	^{89}Y, ^{169}Tm, ^{197}Au
2017	^{59}Co, ^{165}Ho, ^{181}Ta
2018	^{103}Rh, ^{159}Tb, ^{139}La
2019	^{232}Th, ^{238}U ^{208}Pb, ^{112,116,120,124}Sn

Table: NewSUBARU (γ, xn) cross section measurements.

Measurements performed within the **PHOENIX** Collaboration coordinated by **Prof. Hiroaki Utsunomiya, Konan Univ. Japan**

NewSUBARU Japan, SINP China, IFIN-HH Romania, MSU Russia, Oslo University Norway, TU Darmstadt Germany, Universite Libre de Bruxelles Belgium.

Results delivered to the IAEA CRP on Updating the Photonuclear Data Library ▸ Kawano, et al., Nuclear Data Sheets **163**, 109 (2020)

- NewSUBARU (γ, xn) data selected for producing the updated IAEA evaluations. *IFIN-HH evaluations adopted for ^{89}Y, ^{169}Tm, ^{59}Co, ^{165}Ho, ^{181}Ta, ^{103}Rh, ^{159}Tb.*
- have been the basis of recent theoretical calculations: ▸ S.Goriely et al. PRC 102, 064309 (2020)

IAEA CRP data – ^{209}Bi(γ, xn) data

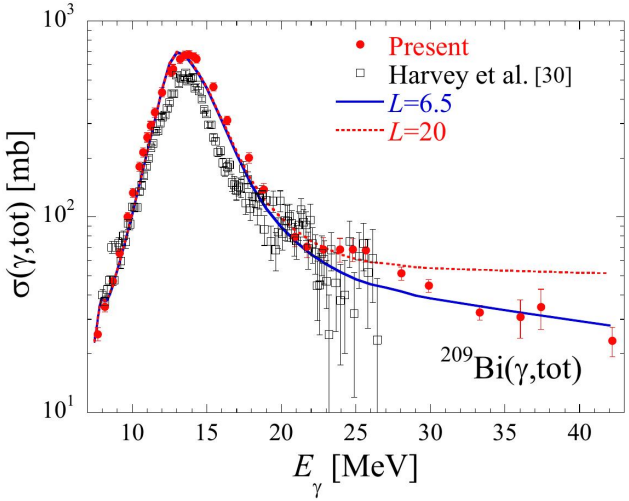

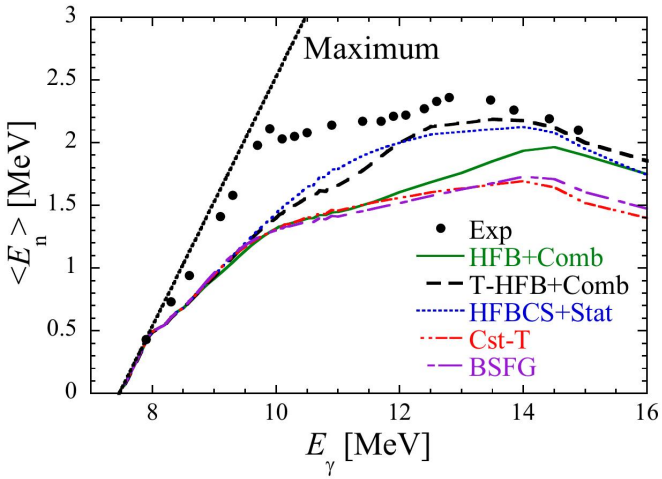

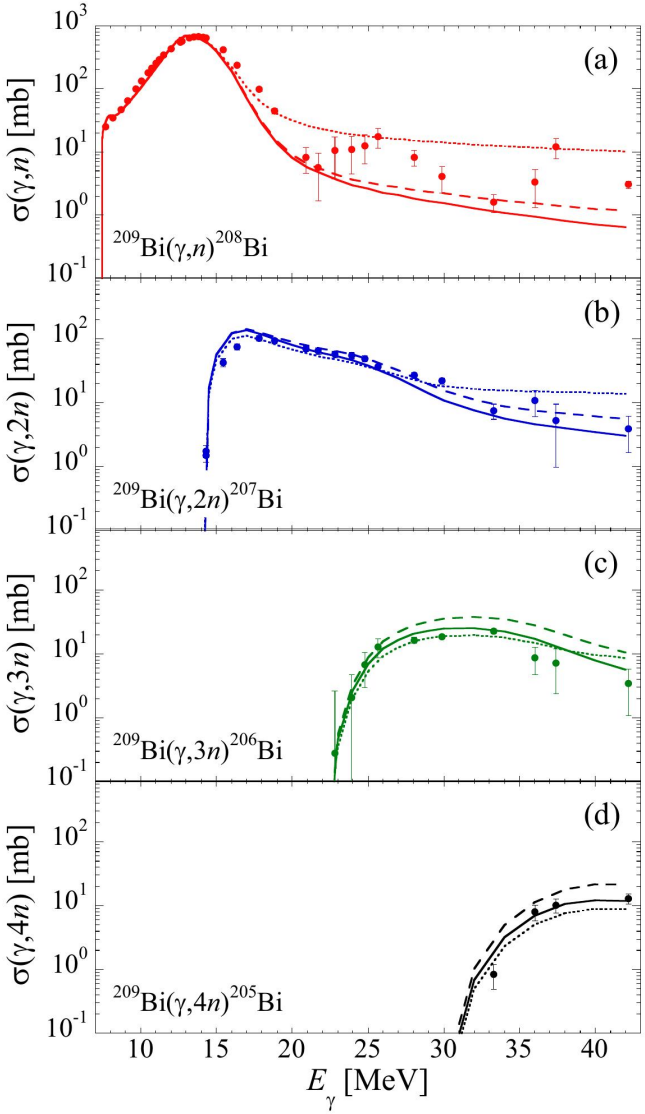

- I.Gheorghe, H.Utsunomiya et al. Phys. Rev. C 96, 044604 (2017)
- Erratum 99, 059901(E) (2019)

IAEA CRP data – T.Kawano et al. Nuclear Data Sheets 163 (2020) 109

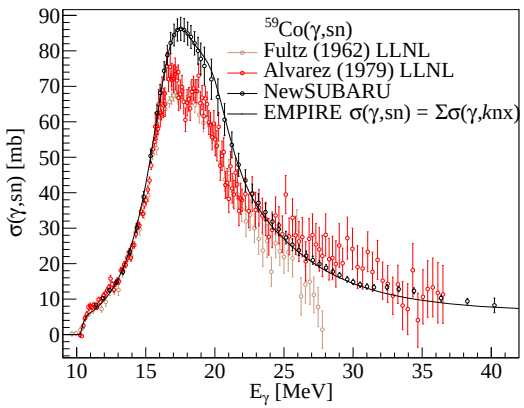

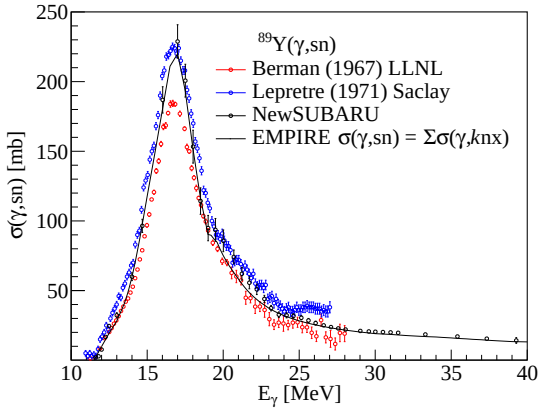

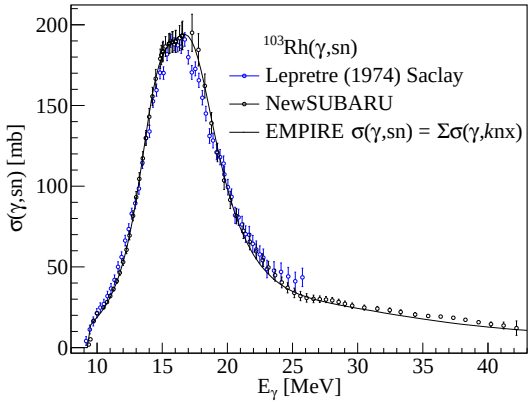

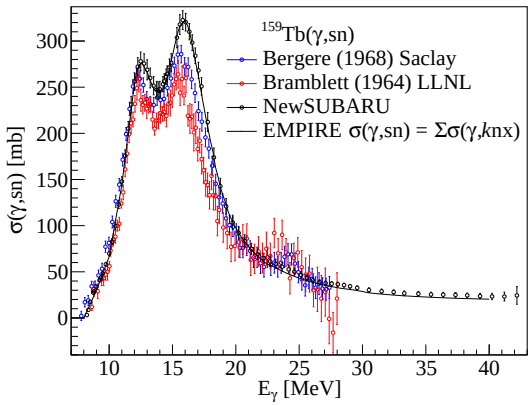

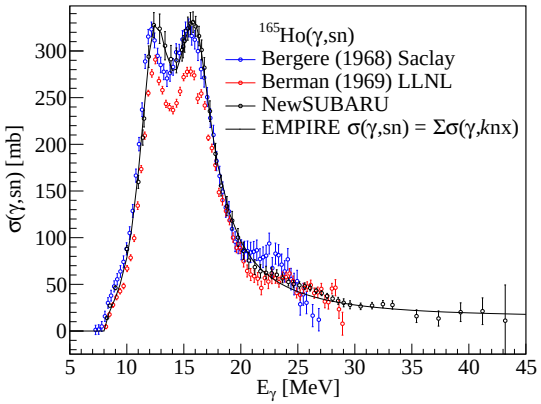

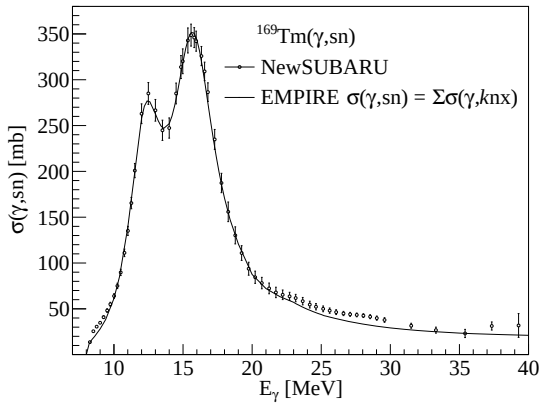

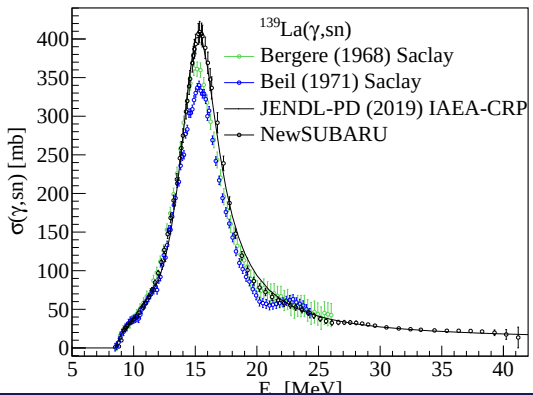

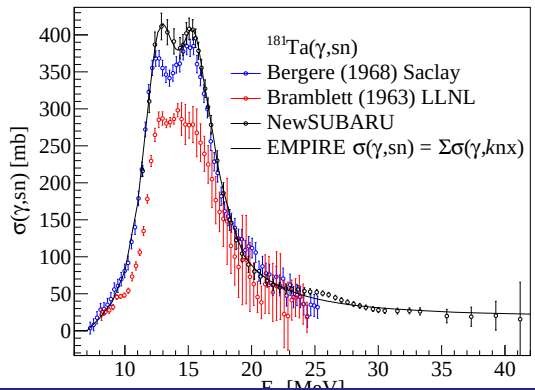

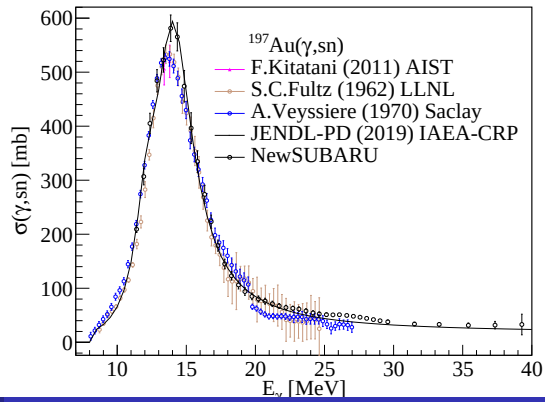

NewSUBARU (γ, xn) cross section measurements *following* IAEA PD CRP

Improved data analysis techniques:

- Monte Carlo model of quasi-monochromatic LCS γ-ray beams:
  - D. Filipescu et al., Spectral distribution and flux of LCS γ-ray beams, NIM A **1047**, 167885 (2023), arXiv:2211.14650
  - D. Filipescu, Monte Carlo simulation of polarization effects in LCS on relativistic electrons, JINST **17** P11006 (2022), arXiv:2210.14669
  - Takashi Ari-Izumi et al., Spatial distribution of collimated LCS γ-ray beams, JINST **18** T06005 (2023), arXiv:2304.08935
- Multiple-firing neutron multiplicity sorting: I. Gheorghe, H. Utsunomiya, et. al, NIMA 1019, 165867 (2021)

New measurements in the GDR energy region:

2015	^{209}Bi, ^{9}Be
2016	^{89}Y, ^{169}Tm, ^{197}Au
2017	^{59}Co, ^{165}Ho, ^{181}Ta
2018	^{103}Rh, ^{159}Tb, ^{139}La
2019	**^{232}Th, ^{238}U** ^{208}**Pb**, ^{112,116,120,124}Sn

Table: NewSUBARU (γ, xn) cross section measurements.

- Photoneutron and photofission measurements on ^{232}Th, ^{238}U Oct 2019
- ^{208}**Pb**, ^{112}Sn, ^{116}Sn, ^{120}Sn, ^{124}Sn Nov-Dec 2019
  Campaign initiated by TUD group of Thomas Aumann.

NewSUBARU synchrotron facility

BL01 LCS γ-ray beam line & GACKO experimental hutch of the Konan University, Kobe, Japan

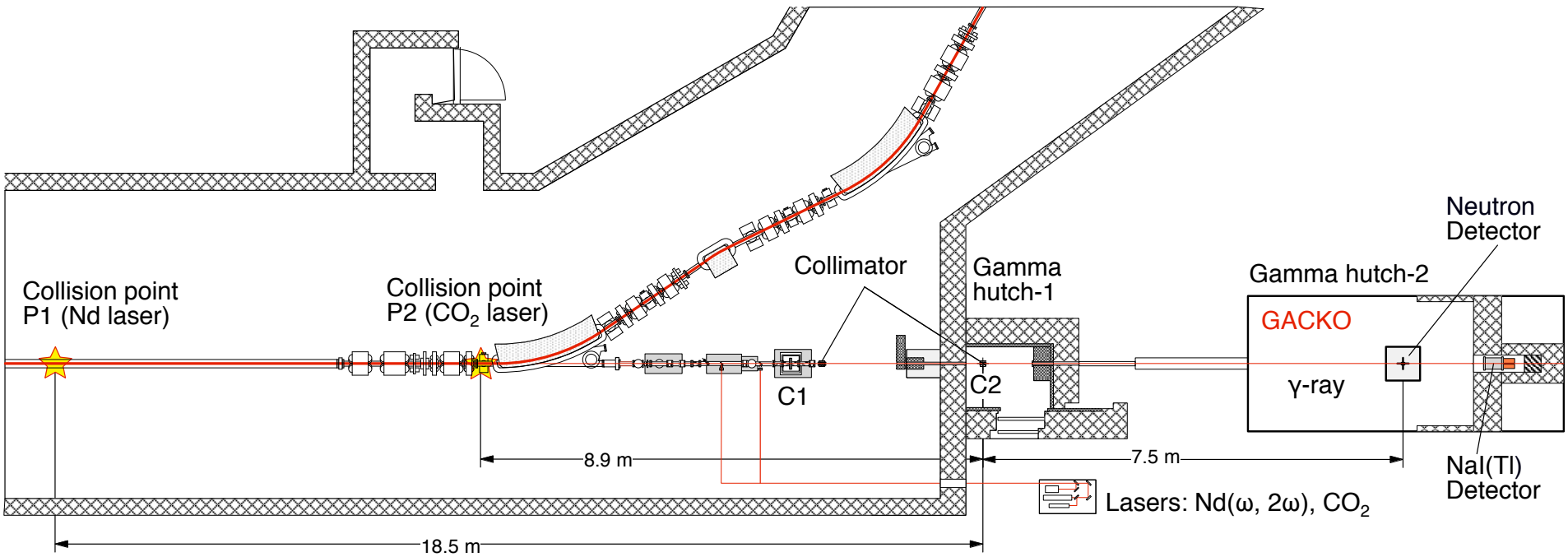

Laser beams are sent head-on against electron beams circulating along a 20 m long straight section of the storage ring. The backscattered γ-ray beam is passed through a double collimation system and sent downstream in the experimental Hutch-2 GACKO (Gamma Collaboration Hutch of Konan University), where the target, neutron detection system and flux and energy profile monitoring systems are placed.

LCS γ-ray beams @ NewSUBARU

1. **Absolute energy**
2. Energy spectra
3. Time structure
4. Flux

Inverse Compton Scattering

"photon accelerator"

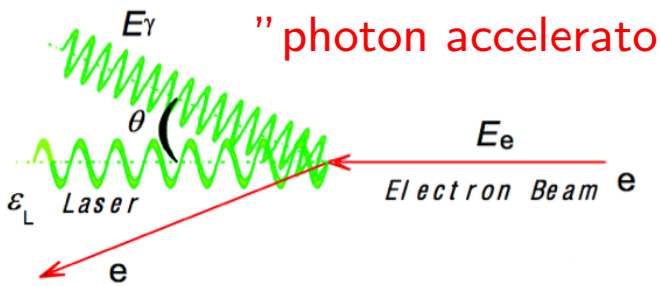

$$E_\gamma = \frac{4\gamma^2 E_p}{1 + (\gamma\theta)^2 + 4\gamma E_p/(mc^2)}.$$

Maximum energy edge for backscattered γs @ θ=0 in head-on collisions is fully determined by:

- laser photon E_p energy: conventional solid state lasers 532 nm and 1064 nm wavelegth
- electron energy $E_e = \gamma \cdot mc^2$
  - variable within 0.5 – 1.5 GeV ▸ Ken Horikawa, NIMA 618, 209 (2010)
  - calibrated by LCS low energy γ-rays generated using CO_2 laser, 10^{-5} precision. ▸ Utsunomiya, IEEE TrNSc 61, 1252 (2014)

Ranges:

- 532 nm laser: 11 – 75 MeV
- 1064 nm laser: 5 – 38 MeV
- fine steps based on electron energy tuning;

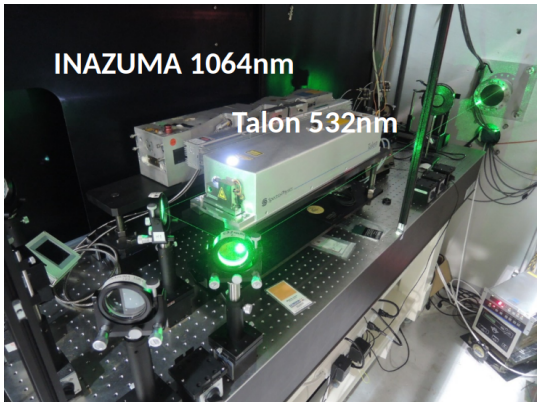

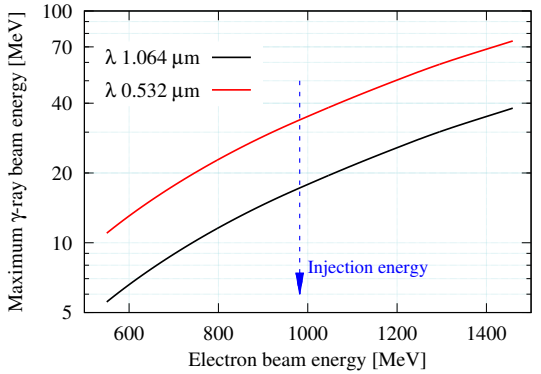

LCS γ-ray beams @ NewSUBARU

1. Absolute energy
2. **Energy spectra**
3. Time structure
4. Flux

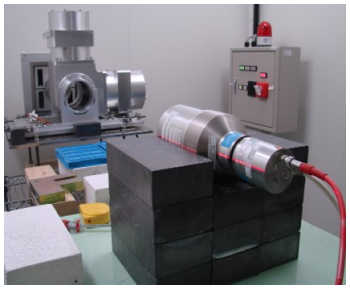

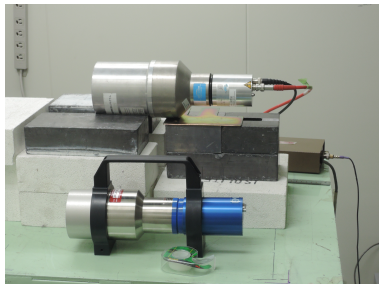

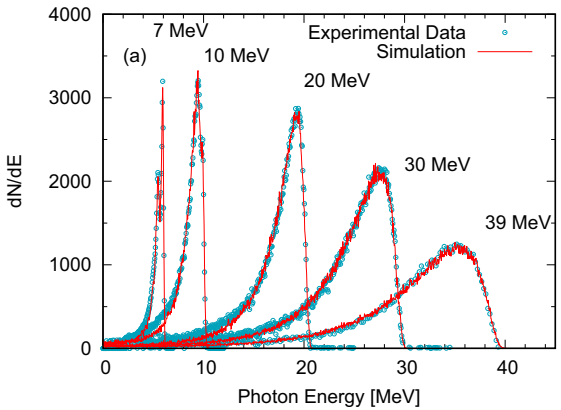

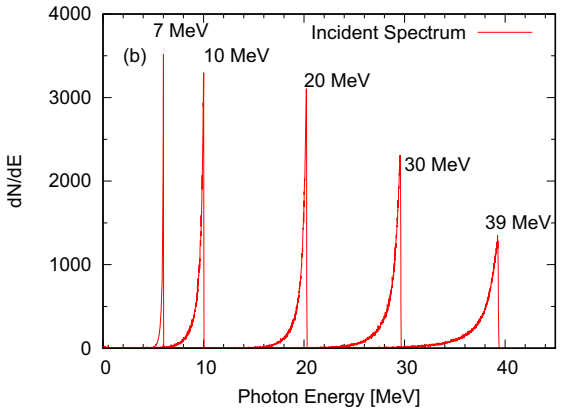

- Quasi-monochromatic spectra 1$\sim$5% FWHM energy spread: selecting by collimation the high-energy, back-scattered Compton spectrum component.
- 3.5" $\times$4.0" $LaBr_3$:Ce monitor detector

Incident spectra obtained by reproducing the experimental detector response through simulations with the `eliLaBr` **LCS γ-ray beam production&transport Monte Carlo simulation code** for characterization of the scattered γ-ray photon beams, considering continuous, unsynchronized laser and electron beams.

- D. Filipescu et al., Spectral distribution and flux of LCS γ-ray beams, NIM A **1047**, 167885 (2023), arXiv:2211.14650
- D. Filipescu, Polarization effects in LCS for producing γ-ray beams, JINST **17** P11006 (2022), arXiv:2210.14669

LCS γ-ray beams @ NewSUBARU

1. Absolute energy
2. Energy spectra
3. **Time structure**
4. Flux

For neutron-multiplicity sorting $E_\gamma > S_{2n}$: Long intervals between consecutive γ-pulses required, on the order of the neutron die-away time in the **moderated** ^{3}He neutron detection array.

- 532 nm laser operated in Q-switch mode at 1 kHz with 40 ns wide photon pulses
- electron beam bunches: 500 MHz freq. and 60 ps width

$\Longrightarrow$ **40 ns wide LCS γ pulses @ laser repetition rate**
each containing several micro-bunches
following fast electron beam time structure.

Background subtraction: laser had also a slow 10 Hz time structure of
80 ms beam-ON / **20 ms beam-OFF**.

Fig: Time structure of 35.41 MeV energy γ-ray beam shown by NaI count rate
(a) 10 Hz beam time structure on 100 ms time scale.
beam-ON interval: 80 γ-ray pulses @ 1 kHz rate
beam-OFF interval: 20 ms flat background rate
(b) time structure on 1 ms time scale

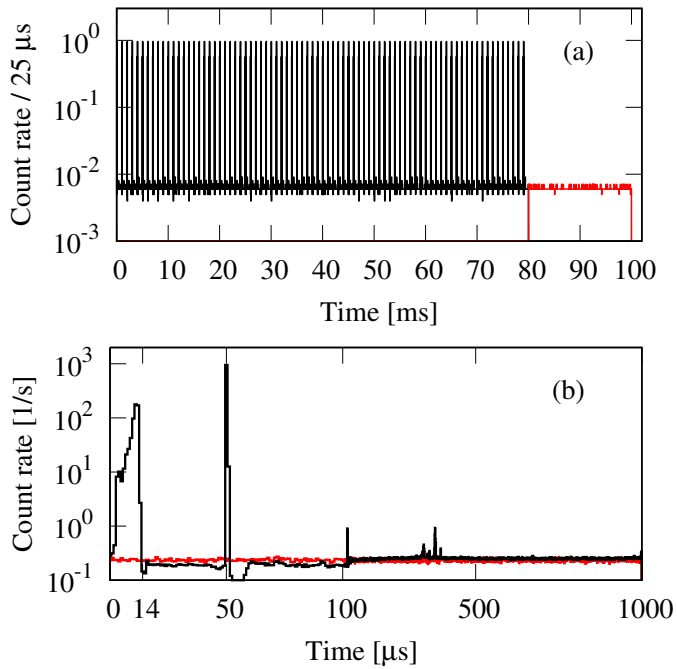

LCS γ-ray beams @ NewSUBARU

1. Absolute energy
2. Energy spectra
3. Time structure
4. **Flux:** $10^4 \sim 10^5$ γ/s

- Electron bunches: 60 ps width & 2 ns interval; Laser pulses: 40∼60 ns width, 1∼25 kHz
  $\Rightarrow$ LCS γ-ray 40∼60 ns width pulses containing tens of 60 ps width micro-bunches.
- Large numbers of laser photons and electrons + small Compton cross section
  $\Rightarrow$ LCS γ multiplicity per pulse:
  Poisson distributed with mean of 10∼20 γ/pulse.
- Large volume NaI detector placed in the beam-dump records sum energy of all photons per bunch $\longrightarrow$ pile-up spectra.
- Pileup method for unfolding and extracting incident flux.

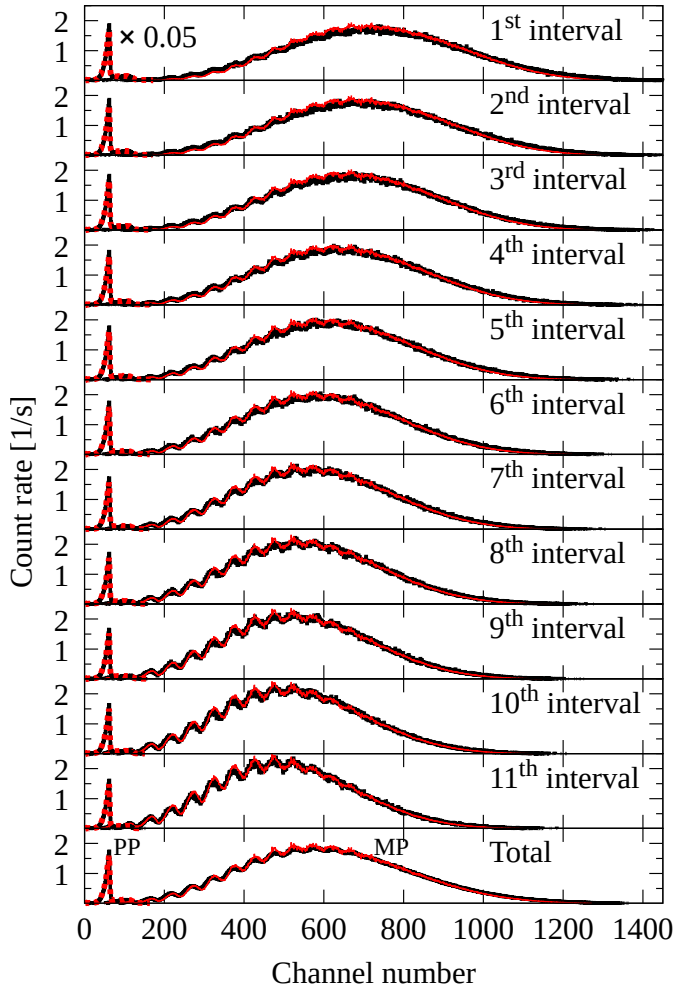

▸ Utsunomiya, NIM A **896**, 103 (2018)

Neutron multiplicity sorting with a Flat Efficiency neutron detector (FED)

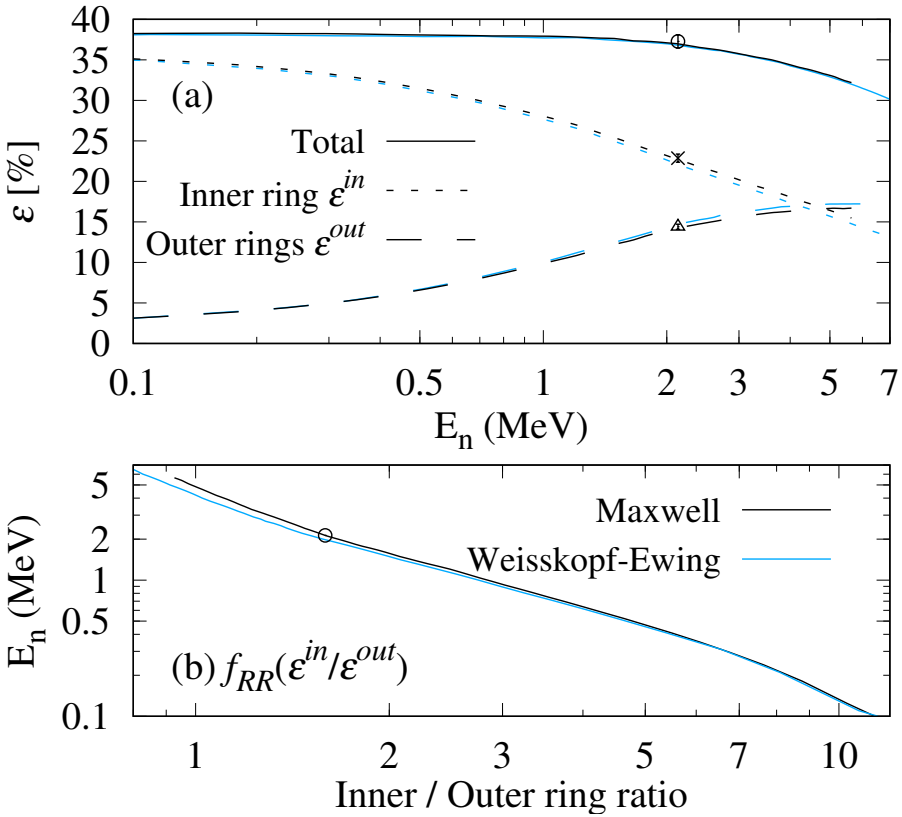

(a) Total detection efficiency (solid) and efficiencies of the inner (dotted) and outer (dashed) rings of the FED obtained by MCNP simulations for Maxwell PFNs spectra (black) (black), neutron evaporation spectra (blue) & experimental ^{252}Cf calibration. (b) Ring ratio curves defined as inner ring / outer rings.

▸ H. Utsunomiya, I. Gheorghe, et. al, NIM A 871, 135-141 (2017)

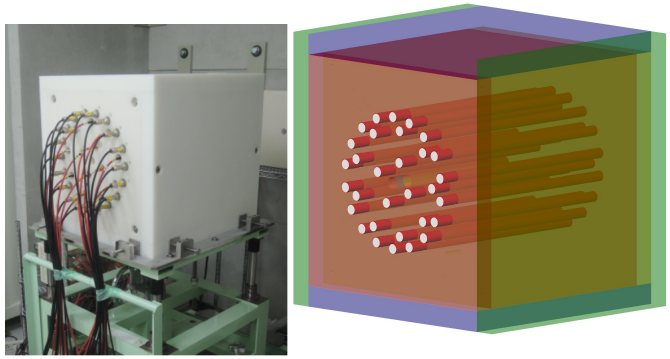

Flat detector response: average $\langle\varepsilon\rangle_{FED} = 36.5\pm1.6\%$; variation 38 $\sim$ 33% in the 10 keV to 5 MeV energy range typical for evaporation photoneutrons and PFN. Measured cross sections are insensitive to the neutron emission spectra.

neutron fold	efficiency
1 neutron	ε=$\sim$38%
2 neutrons	ε^2=$\sim$14%
3 neutrons	ε^3=$\sim$5.5%
4 neutrons	ε^4=$\sim$2%
i neutrons	ε^i=small

Updated neutron-multiplicity sorting method

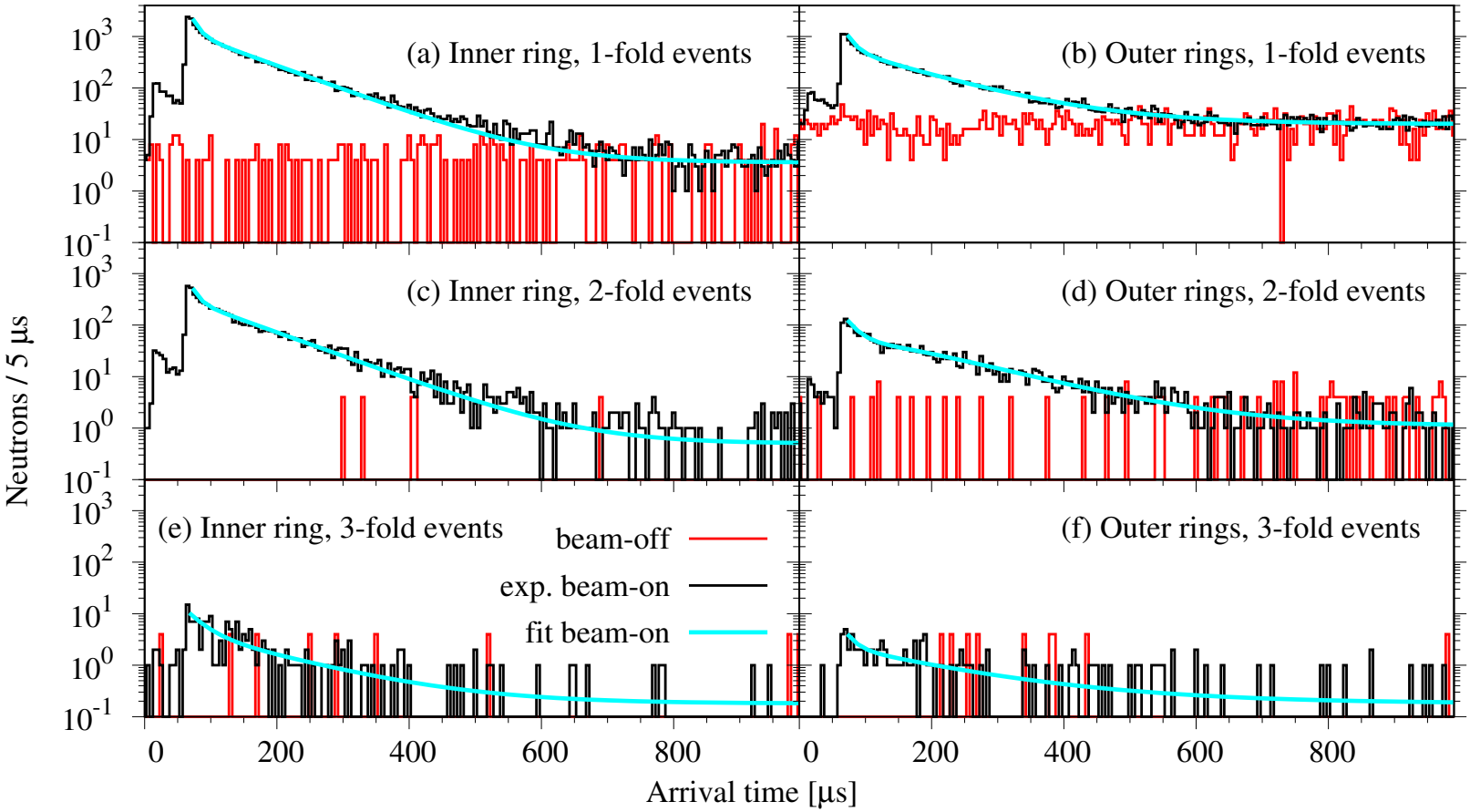

Figure: Arrival-time distributions of neutrons recorded by the FED neutron-multiplicity sorting experiments. Experimental neutron counts recorded during beam-on (black) and beam-off (red) and the best fit to the beam-on distribution (cyan).

Experimental observables:

- ***i*-fold cross section** N_i = the number of i-fold photoneutron events recorded per incident photon and target nucleus:

$$N_i = \frac{\sum_t (n_i^{in}[t] + n_i^{out}[t])/i}{N_\gamma n_T \xi}$$

  where $n_i^{in}[t]$ and $n_i^{out}[t]$ are the background subtracted arrival time histograms for neutrons detected in i-fold events by the inner ring and by the summed two outer rings, respectively. n_T is the concentration of target nuclei, N_γ is the incident photon number for the total irradiation time and $\xi = [1 - \exp(-\mu L)]/\mu$ is a thick target correction factor given by the target thickness L and attenuation coefficient μ.

- ***i*-fold average neutron energies** E_i determined by the RR method as $E_i = f_{RR}(\sum_t n_i^{in}[t] / \sum_t n_i^{out}[t])$.

Direct Neutron Multiplicity (DNM) method

$$N_i = \sum_{x=i}^{\mathrm{N}} \sigma_{\gamma,xn} \cdot {}_xC_i \varepsilon^i (1-\varepsilon)^{x-i},$$

$$E_i = \sum_{x=i}^{\mathrm{N}} E_{\gamma,xn} \cdot F^*_{ix},$$

where the F^*_{ix} factor is defined as:

$$F^*_{ix} = \sigma_{\gamma,xn} \cdot {}_xC_i \varepsilon^i (1-\varepsilon)^{x-i} / N_i.$$

Operates under the single firing condition based on a flat-efficiency neutron detection system.

▸ H. Utsunomiya, I. Gheorghe, et. al, NIM A 871, 135-141 (2017)

Multiple Firing (MF) method

Statistical treatment of multiple firing neutron coincidence events. We use the `minuit` package of `ROOT` for performing a χ^2 minimization procedure to determine the *multiple firing* corrected $\sigma^{MF}_{\gamma,xn}$ photoneutron cross sections and $E^{MF}_{\gamma,xn}$ average neutron spectra energies from the measured N_i i-fold cross sections and E_i average energies.

- free parameters: $\sigma^{MF}_{\gamma,xn}$ and $E^{MF}_{\gamma,xn}$ ($x = 1$ to N)
- fixed parameters: target characteristics (n_T, ξ), multiplicity distribution of incident LCS γ-rays ($\langle N_\gamma(k) \rangle$, $p_w(k)$), number of incident multi-photon γ-ray pulses ($N_{\gamma p}$)

▸ I. Gheorghe, H. Utsunomiya, et. al, NIMA 1019, 165867 (2021)

Energy unfolding - procedure

Although the spectral density concentration in the maximum energy region of the spectra makes LCS γ-ray beams ideal for investigating photonuclear excitation functions,

- the **measured** cross sections are the folding between the excitation function and the beam spectral distribution:

$$\sigma^{\text{fold}}_{\gamma,\,kn}(E_m) = \xi \cdot \int_0^{E_{mi}} L(E_\gamma, E_m)\sigma_{\gamma,kn}(E_\gamma)\, dE,$$

Iterative energy unfolding procedure ▸ T. Renström PRC 98, 054310 (2018)

$$\begin{pmatrix} \sigma^{\text{fold}}_{\gamma,\,kn\,1} \\ \sigma^{\text{fold}}_{\gamma,\,kn\,2} \\ \vdots \\ \sigma^{\text{fold}}_{\gamma,\,kn\,\mathtt{Nf}} \end{pmatrix} = \xi \cdot \begin{pmatrix} L_{11} & L_{12} & \dots & L_{1\mathtt{Mf}} \\ L_{21} & L_{22} & \dots & L_{2\mathtt{Mf}} \\ \vdots & \vdots & \ddots & \vdots \\ L_{\mathtt{Nf}1} & L_{\mathtt{Nf}2} & \dots & L_{\mathtt{NfMf}} \end{pmatrix} \cdot \begin{pmatrix} \sigma_{\gamma,\,kn\,1} \\ \sigma_{\gamma,\,kn\,2} \\ \vdots \\ \sigma_{\gamma,\,kn\,\mathtt{Mf}} \end{pmatrix}$$

Photoneutron ^{208}Pb collaboration

- Hiroaki Utsunomiya, Takashi Ari-izumi (*Konan University, Japan*)
- Thomas Aumann, Heiko Scheit, Dmytro Symochko, Patrik van Beek, Martin Baumann, Philipp Kuchenbrod, Nikolina Lalić
  (*Institut für Kernphysik, Technische Universität Darmstadt, Germany*)
- Ioana Gheorghe (*IFIN-HH, Romania*)
- Tomas Eriksen, Fardous Raez, Vetle Wegner Ingeberg, Frank L. Bello Garrote, Line G. Pedersen, Wanja Paulsen (*Department of Physics, University of Oslo, Norway*)
- Sergey Belyshev (*Lomonosov Moscow State University, Russia*)
- Shuji Miyamoto (*LASTI, University of Hyogo, Japan*)
- Stephane Goriely (*Université Libre de Bruxelles, Belgium*)

Existing data for ^{208}Pb(γ, xn) cross section

Systematic discrepancies between Saclay and Livermore photoneutron cross sections:

$$\sigma_{SAC}(\gamma, abs) > \sigma_{LIV}(\gamma, abs)$$
$$\sigma_{SAC}(\gamma, n) > \sigma_{LIV}(\gamma, n)$$
$$\sigma_{SAC}(\gamma, 2n) < \sigma_{LIV}(\gamma, 2n)$$

A. Veyssiere et al.,
Nucl. Physics A159, 561 (1970).
R.R. Harvey et al.,
Phys. Rev. 136, 126 (1964).

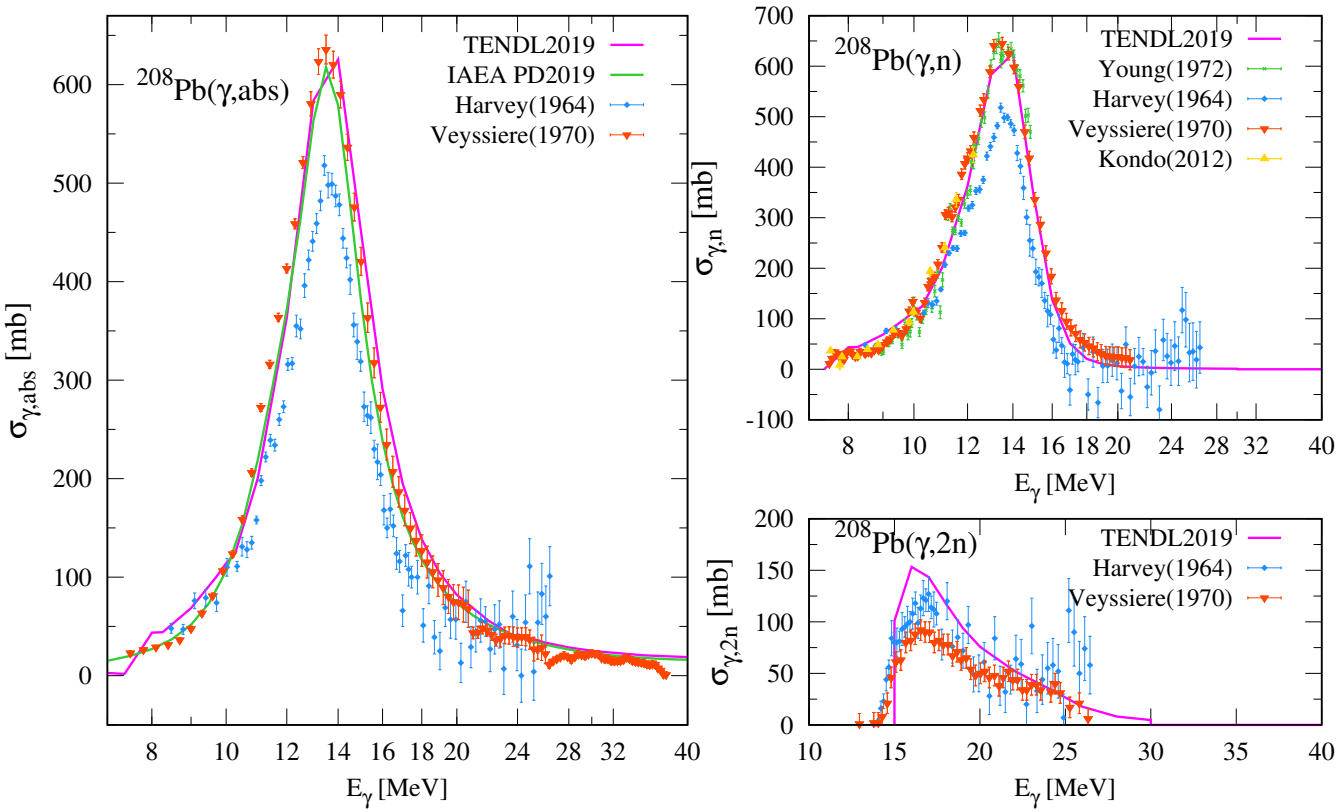

The 1999 and 2019 IAEA PD ^{208}Pb evaluations follow the recommendation of Berman et al. PRC 36, 1286 (1987) of lowering the Saclay data by 7% and increasing the Livermore results by 22%, although a single renormalization factor fails to simultaneously solve the inconsistencies for both the (γ, n) and (γ, 2n) channels.

LCS γ-ray beam diagnostics at NewSUBARU - **Energy spectra**

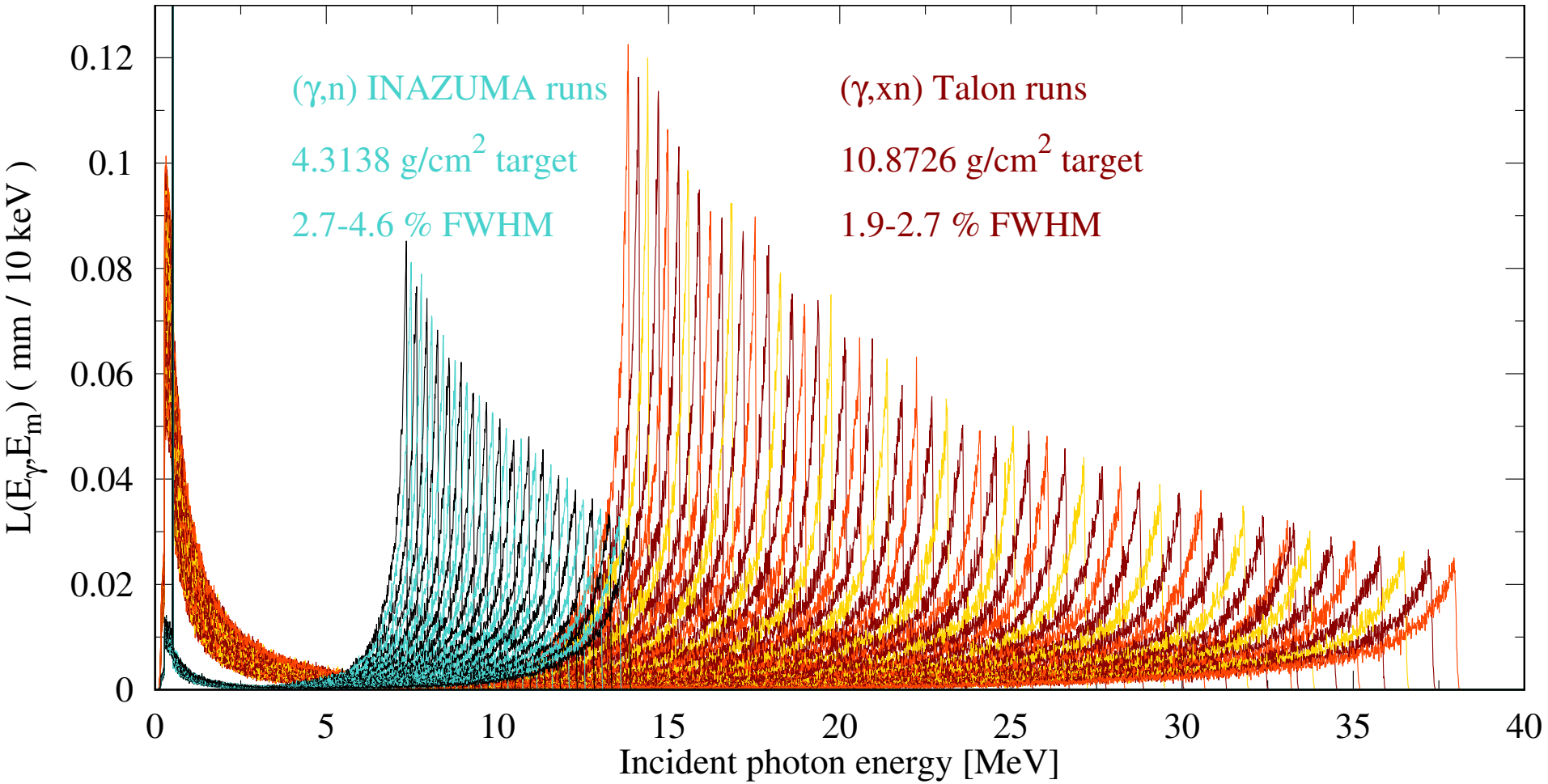

In order to model the secondary photon production in the target and asses their contribution to the measured reaction yield, we use the $L(E_\gamma, E_m)$ distribution defined as the average path length per unit energy traveled through the target by a E_γ photon in a LCS γ-ray beam of E_m maximum energy.

Neutron coincidence events: i-fold cross sections and N_i average neutron energies

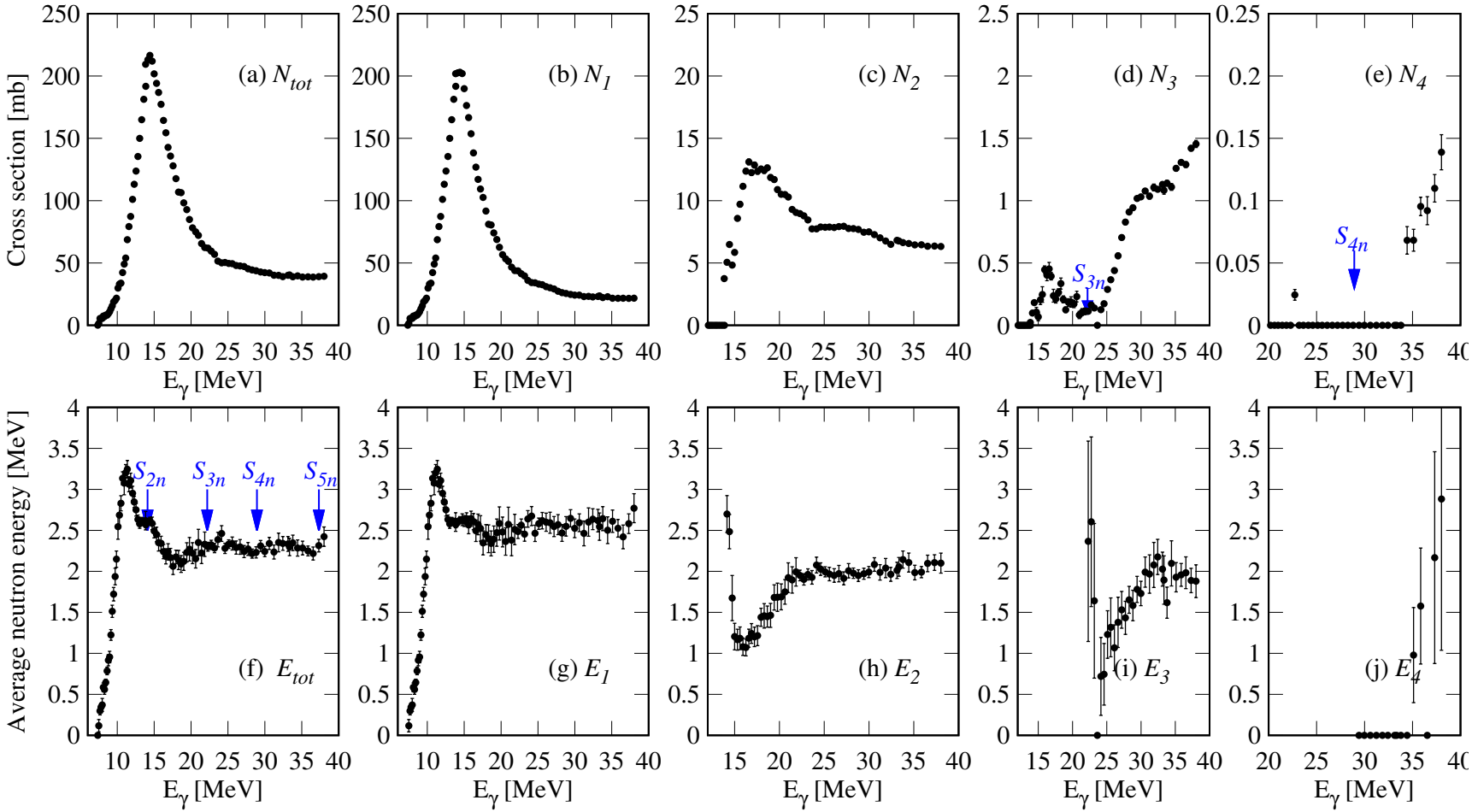

Figure: (a-e) Experimental N_i i-fold cross sections and (f-j) E_i average neutron energies for single (1-fold), double (2-fold), triple (3-fold) and quadruple (4-fold) coincidence events and for total neutron events (N_{tot}, E_{tot}) in the ^{208}Pb(γ, xn) reactions. Error bars are determined by statistical fluctuations of i-fold neutron counts.

Average energies of (γ, xn) photoneutrons for ^{208}Pb

(a-d) Experimental average energies of neutrons emitted in ^{208}Pb(γ, xn) reactions with x = 1 – 4, obtained by:

- DNM method ($E^{DNM}_{\gamma, xn}$ ○)
- MF method ($E^{MF}_{\gamma, xn}$ •)

and the average energy of the total neutron spectra (E_{tot})

Dash-dotted lines correspond to maximum energies given by kinematics $(A-1)/A \cdot (E_\gamma - S_{xn})$, where A is the mass number.

(e-h) The $\varepsilon^{MF}_{\gamma, xn} = \varepsilon(E^{MF}_{\gamma, xn})$ detection efficiency for each ^{208}Pb(γ, xn) reaction, along with $\varepsilon_{tot} = \varepsilon(E_{tot})$ (orange band).

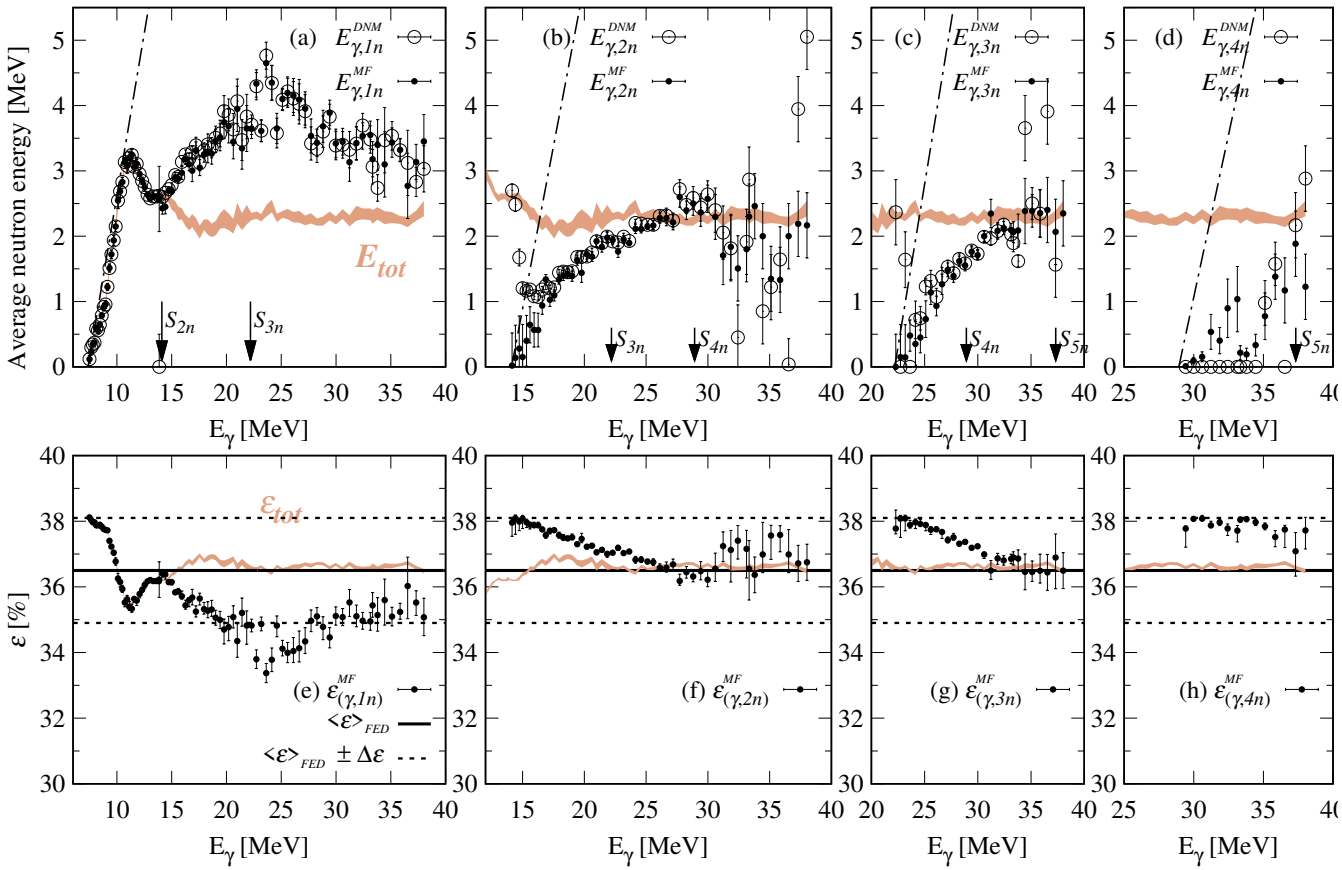

Experimentally extracted $\varepsilon^{MF}_{\gamma, xn}$ detection efficiencies generally close to the ε_{tot} and to the energy averaged FED detection efficiency $\langle\varepsilon\rangle_{FED}$, with differences < 1 % $\Longrightarrow$ **robust and highly accurate determination of (γ, xn) cross sections, with low sensitivity to the neutron emission spectra!**

Preliminary ^{208}Pb(γ, *tot*) cross sections

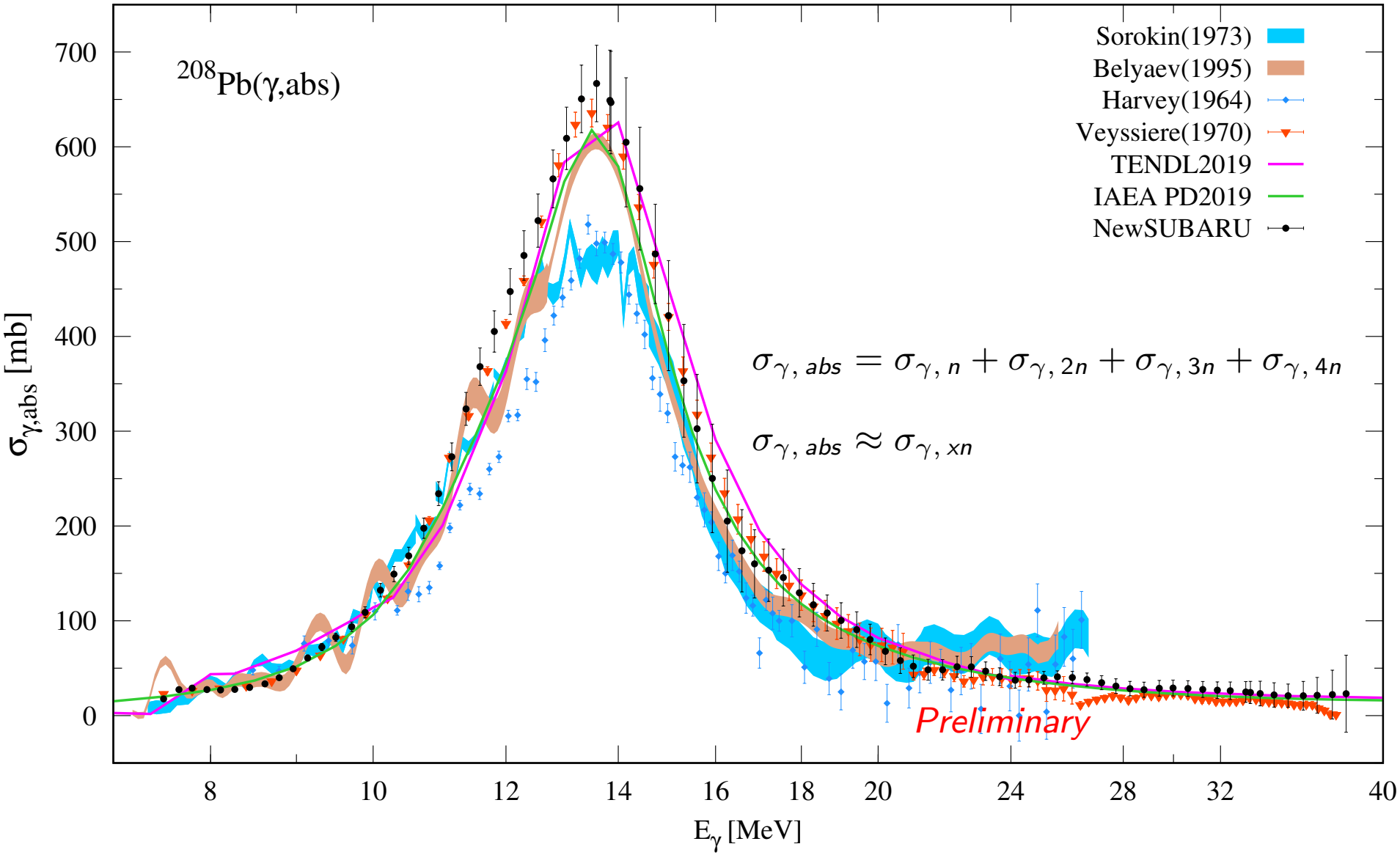

Preliminary ^{208}Pb(γ, xn) cross sections

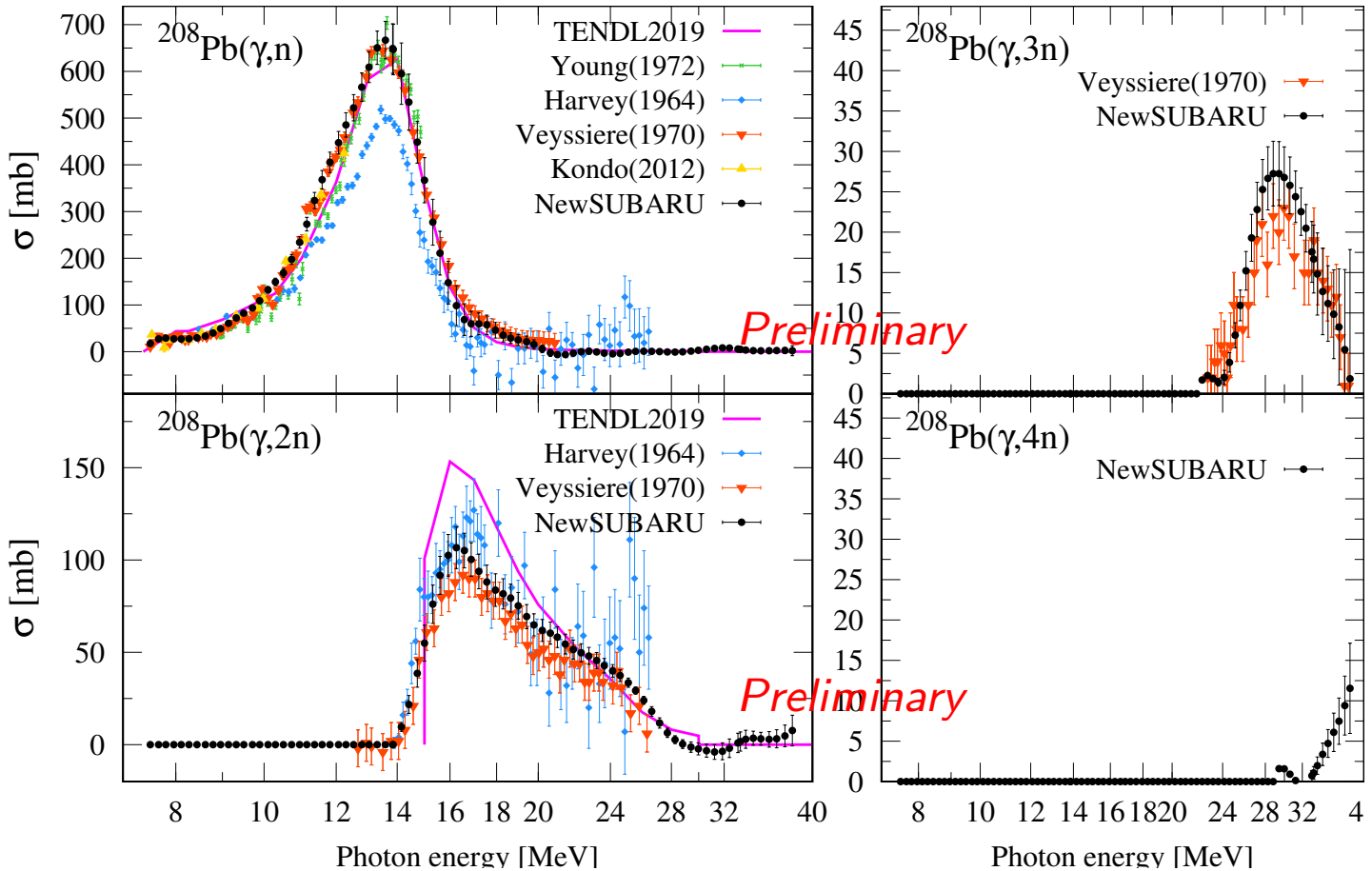

Summary and further work to be done on the ^{208}Pb(γ, xn) data analysis

Continued the IAEA CRP photoneutron campaign at NewSUBARU with ^{208}Pb(γ, xn) measurements in the S_n to 38 MeV energy range.
Preliminary results:

$$\sigma_{SAC}(\gamma, abs) \approx \sigma_{NewSUBARU}(\gamma, abs) > \sigma_{LIV}(\gamma, abs)$$
$$\sigma_{SAC}(\gamma, n) \approx \sigma_{NewSUBARU}(\gamma, n) > \sigma_{LIV}(\gamma, n)$$
$$\sigma_{SAC}(\gamma, 2n) < \sigma_{NewSUBARU}(\gamma, 2n) < \sigma_{LIV}(\gamma, 2n)$$

Similar to the behavior observed in our previous ^{209}Bi study, a non-statistical emission of high energy neutrons was registered starting in the vicinity of the neutron emission threshold up to $\sim$ 11 MeV excitation energy.
Further work on data analysis:

- Improve neutron energy determination at excitation energies between S_n and S_{2n}, at the transition from neutron emission to few discrete available states in the residual to a statistic decay;
- Unfolding of average neutron energy data;
- Investigate resonant structures in the low-energy part of the GDR using the Taylor expansion method routinely used in (γ,n) cross section measurements below S_{2n}
  - H. Utsunomiya, et. al, PRC 92, 064323 (2015)

Collaboration on the ^{238}U and ^{232}Th study

- Hiroaki Utsunomiya, Takashi Ari-izumi (*Konan University, Japan*)
- Gongtao Fan, Hongwei Wang (*SLEGS, Shanghai Advanced Research Institute, Chinese Academy of Sciences, China*)
- Dan Filipescu, Ioana Gheorghe (*IFIN-HH, Romania*)
- Katsuhisa Nishio, Fumi Suzaki, Kentaro Hirose (*Advanced Science Research Center, Japan Atomic Energy Agency, Japan*)
- Tsutomu Ohtsuki, Makoto Inagaki (*Institute for Integrated Radiation and Nuclear Science, Kyoto University, Japan*)
- Konstantin Stopani (*Lomonosov Moscow State University, Russia*)
- Anabella Tudora (*University of Bucharest, Bucharest, Romania*)
- Marianne Bjørøen (*Department of Physics, University of Oslo, Norway*)
- Yiu-Wing Lui (*Cyclotron Institute, Texas A&M, USA*)
- Shuji Miyamoto (*LASTI, University of Hyogo, Japan*)

Photofission at the GDR energy region

- The photoabsorption cross section is known to be dominated by the electric dipole (E1) mode in the γ-ray energy region of $\sim S_n$ to $\sim$20 MeV characterizing the well-known Giant Dipole Resonance (GDR).
- Starting with medium mass nuclei, the height of the Coulomb barrier restricts charged particle emission decays of the GDR.
- For actinide nuclei, the photoabsorption cross section can thus be well approximated with the sum cross section of the photofission and photoneutron (γ, n), $(\gamma, 2n)$, ... reactions.
- A simultaneous reproduction of the competing photoneutron (γ, n), $(\gamma, 2n)$, ... as well as the first- (γ, f), second- (γ, nf), ... chances photofission cross sections can be a valuable tool in validating the consistency and reliability of the fission barrier parameters and the states at super- and hyper-deformations.

- Starting with the 1960's, photoneutron cross section measurements in the GDR region had been routinely performed at the Saclay and Livermore positron in flight annihilation facilities by multiplicity sorting of coincidence neutron detection events from (γ, xn) reactions with $x = 1, 2, 3$. Many of the existing data on photoabsorption cross sections in the GDR region have been produced at these two facilities.
- Systematic discrepancies still unresolved are however present between the Saclay and Livermore data sets
- The main experimental challenge in the Saclay and Livermore neutron multiplicity sorting investigations of photonuclear reactions in the GDR region was to discriminate the photofission emission from the photoneutron one for incident photon energies above the neutron separation energy.

LCS γ-ray beams - energy, time structure, flux

- LCS γ-ray beams with energies from 5.87 to 20.14 MeV.
- 40 energy electron beam energy values between 589.89 and 1071.78 MeV.
- LCS γ-ray beam repetition rate: 1 kHz.
- 10 Hz frequency pulsed macro-time structure of 80 ms beam-on followed by 20 ms beam-off.
- Mean number of photons per pulse varied between 5 and 15, corresponding to incident photon fluxes of $4 - 12 \cdot 10^3$ γ/s.

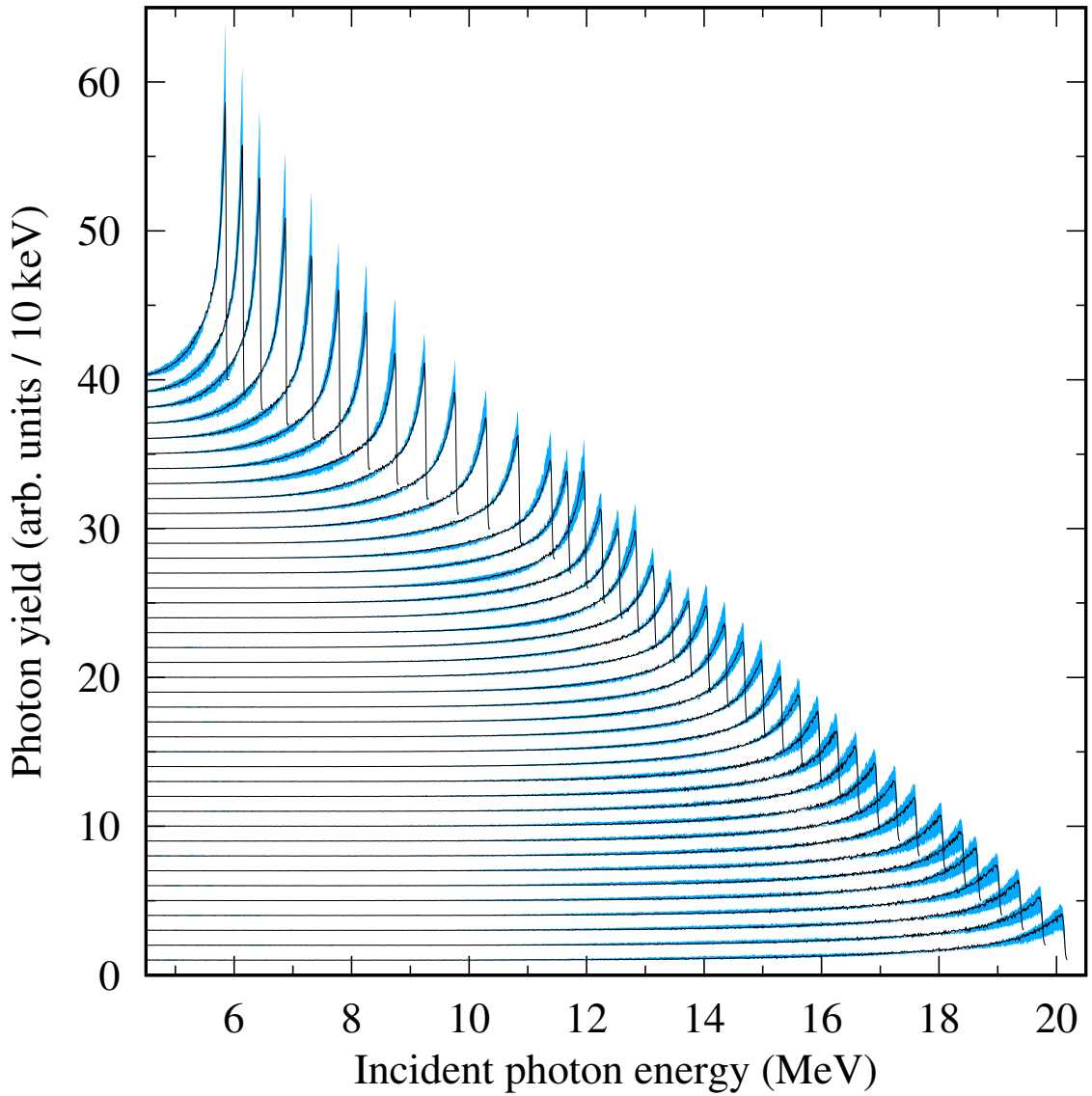

Actinide targets and LCS γ-ray beam spot size

The LCS γ-ray beams irradiated target materials of 8.62 g ThO_2 and 4.06 g U_3O_8 encapsulated in pure-aluminum cylindrical containers.
Areal density:

- ^{232}Th 17.15 g/cm^2
- ^{238}U 8.08 g/cm^2

Contributions from the Al container and from oxygen nuclei above their corresponding neutron emission thresholds have been measured independently using an empty container and a H_2O target in an Al cylinder with Kapton windows, respectively.

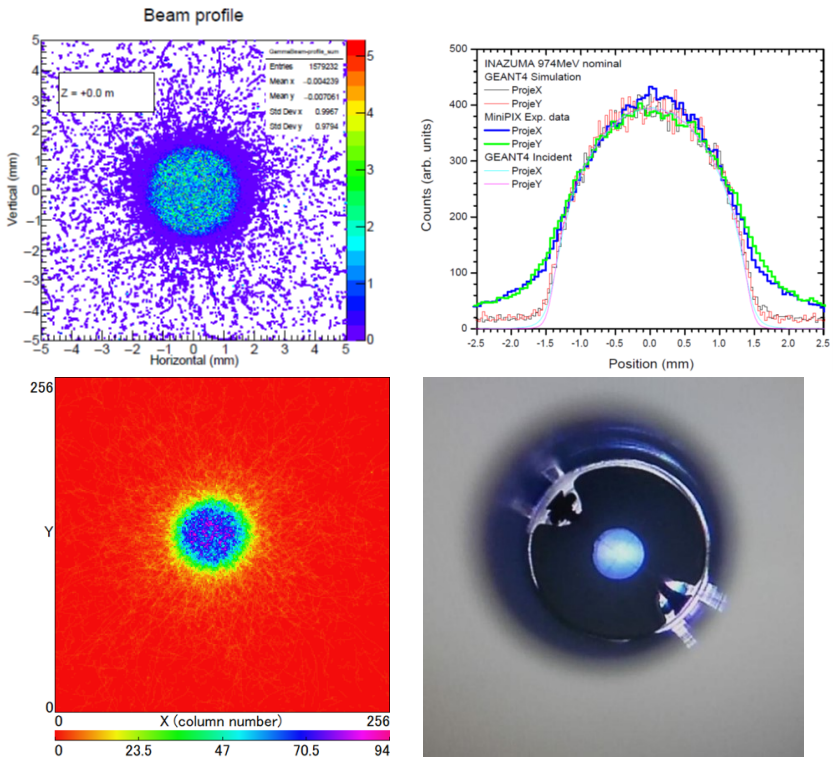

Target diameter 8 mm
γ-ray beam spot diameter $\sim$ 4 mm

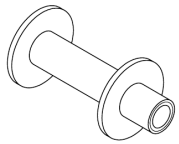

Spatial profiles of collimated laser Compton-scattering γ-ray beam

▸ Takashi Ari-Izumi et al., 2023 JINST 18 T06005

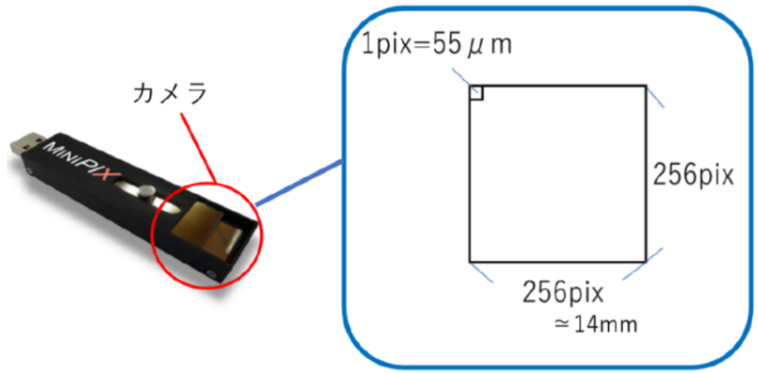

Neutron multiplicity counting

Figure: Arrival-time distributions of neutrons recorded by the FED in photon-induced reactions on ^{238}U at 18.67 MeV.
Experimental neutron counts recorded during:

beam-on (black)
beam-off (blue)

are displayed for:

- (a) 1-fold
- (b) 2-fold
- (c) 3-fold
- (d) 4-fold
- (e) 5-fold
- (f) 6-fold
- (g) 7-fold

neutron events.

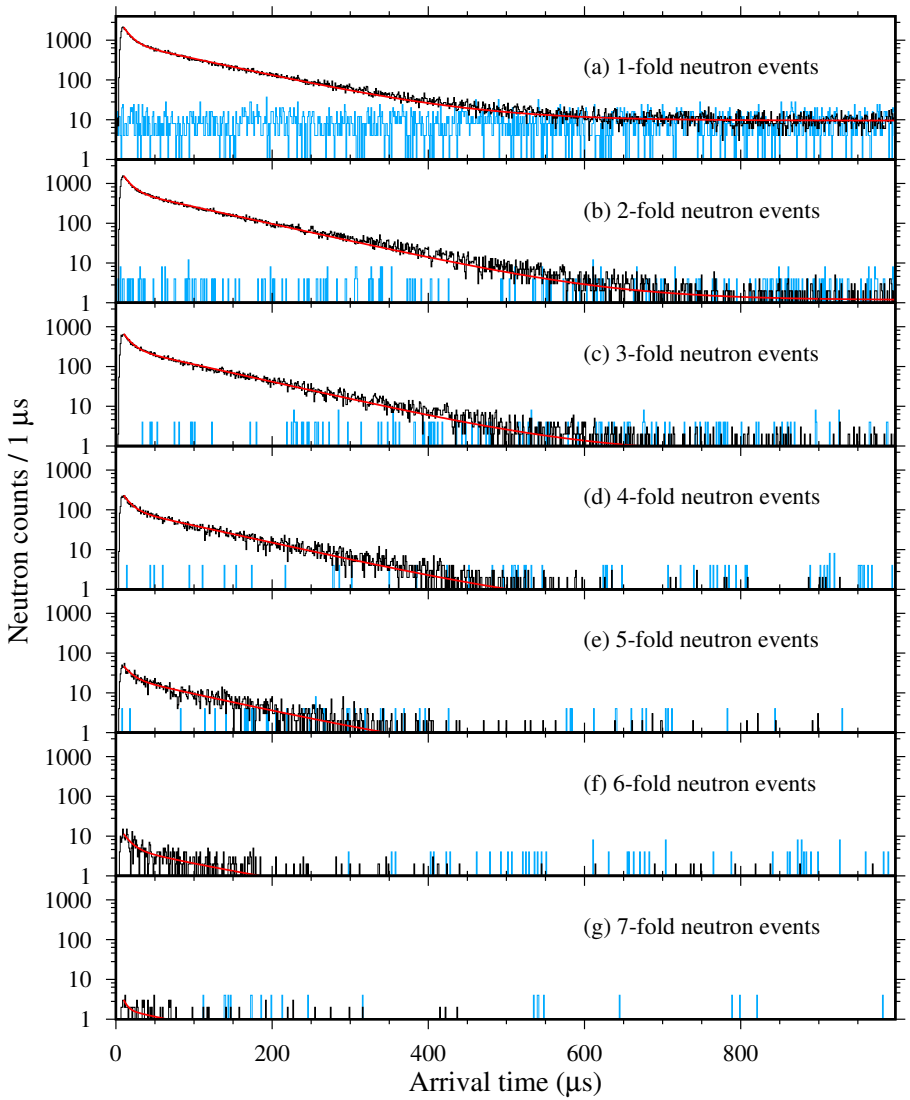

Photoneutron and photofission contributions to neutron coincidence events

Competing reactions for actinide target irradiation with a γ-ray beam of energy $S_{2n} < E < S_{3n}$:

- photoneutron $(\gamma,\ n)$, $(\gamma,\ 2n)$
- photofission $(\gamma,\ f\ in)$ with emission of i neutrons, $0 \leq i \leq \nu_{max} \simeq 9$

For non-unity detection efficiency ε and *single-firing* conditions (no more than one nuclear reaction induced by the same photon pulse), the recorded N_1, N_2, ... N_k coincidences of 1, 2, respectively k neutrons are expressed as:

k-fold coincidence events	contributing reactions
$N_1 \sim \sigma_{(\gamma,\,n)} \cdot \varepsilon + \sigma_{(\gamma,\,2n)} \cdot 2\varepsilon(1-\varepsilon) + \sigma_{(\gamma,\,f)} \sum_{i=1}^{\nu_{max}} P_i \cdot {}_iC_1 \varepsilon (1-\varepsilon)^{i-1}$	$(\gamma,\ n)$, $(\gamma,\ 2n)$, $(\gamma,\ f\ in)$ with i ≥ 1
$N_2 \sim \sigma_{(\gamma,\,2n)} \cdot \varepsilon^2 + \sigma_{(\gamma,\,f)} \sum_{i=2}^{\nu_{max}} P_i \cdot {}_iC_2 \varepsilon^2 (1-\varepsilon)^{i-2}$	$(\gamma,\ 2n)$, $(\gamma,\ f\ in)$ with i ≥ 2
$N_k \sim \sigma_{(\gamma,\,f)} \sum_{i=k}^{\nu_{max}} P_i \cdot {}_iC_k \varepsilon^k (1-\varepsilon)^{i-k}$	$(\gamma,\ f\ in)$ with i ≥ 3

with P_i the probability to emit i neutrons in a fission event.

CHALLENGES:

- Because of non-unity detection efficiency, maximum order of detected neutrons is lower than $\nu_{max} \implies$ incomplete system of k equations with ν_{max} variables!
- Discrimination of the photoneutron $(\gamma,\ n)$, $(\gamma,\ 2n)$ and photofission contributions to the 1- and 2-fold neutron coincidence events.

SOLUTION: Description for the PFN multiplicity emission!

Energy dependent multiple-firing (MF) sorting method

Statistical treatment of multiple firing neutron coincidence events, originally developed for photoneutron reactions only ▸ I. Gheorghe, H. Utsunomiya, et. al, NIMA 1019, 165867 (2021) as a follow-up for the Direct Neutron Multiplicity (DNM) sorting method which operates in *single-firing* conditions ▸ H. Utsunomiya, I. Gheorghe, et. al, NIM A 871, 135-141 (2017). Here we extended the method to include photofission reactions described by the Gaussian distribution of PFN multiplicities given by Terrell.

For each experimental point, we considered:

- the open (γ, xn) reaction channels, where the maximum x multiplicity $\mathtt{N}$ is determined by the incident photon energy. For the energy range here investigated, $\mathtt{N}$ varied from 0 to 3. Each reaction channel is characterized by:
  - $\sigma_{\gamma,xn}$ cross section;
  - $E_{\gamma,xn}$ average photoneutron energy.
- the (γ, $f\,xn$) reactions, where x takes values from 1 to $\nu_{max} \simeq 9$. The photofission channel is characterized by:
  - $\sigma_{\gamma,F}$ total photofission cross section;
  - $\overline{\nu}$ and σ parameters of the Gaussian PFN multiplicity distribution;
  - $E_{\gamma,F}$ average energy of PFN. Note that the same value is considered for all PFN emission multiplicities, regardless of the fission chance.

Minimization constraints:

- $\sigma_{\gamma,xn}$ free parameters
- $E_{\gamma,xn}$ free parameters
- $\sigma_{\gamma,F}$ free parameter
- PFN $\overline{\nu}$ free parameter
- PFN $E_{\gamma,F}$ free parameter
- PFN σ constrained to a linearly energy dependent value.

Preliminary results - ^{238}U and ^{232}Th photoneutron and photofission cross sections

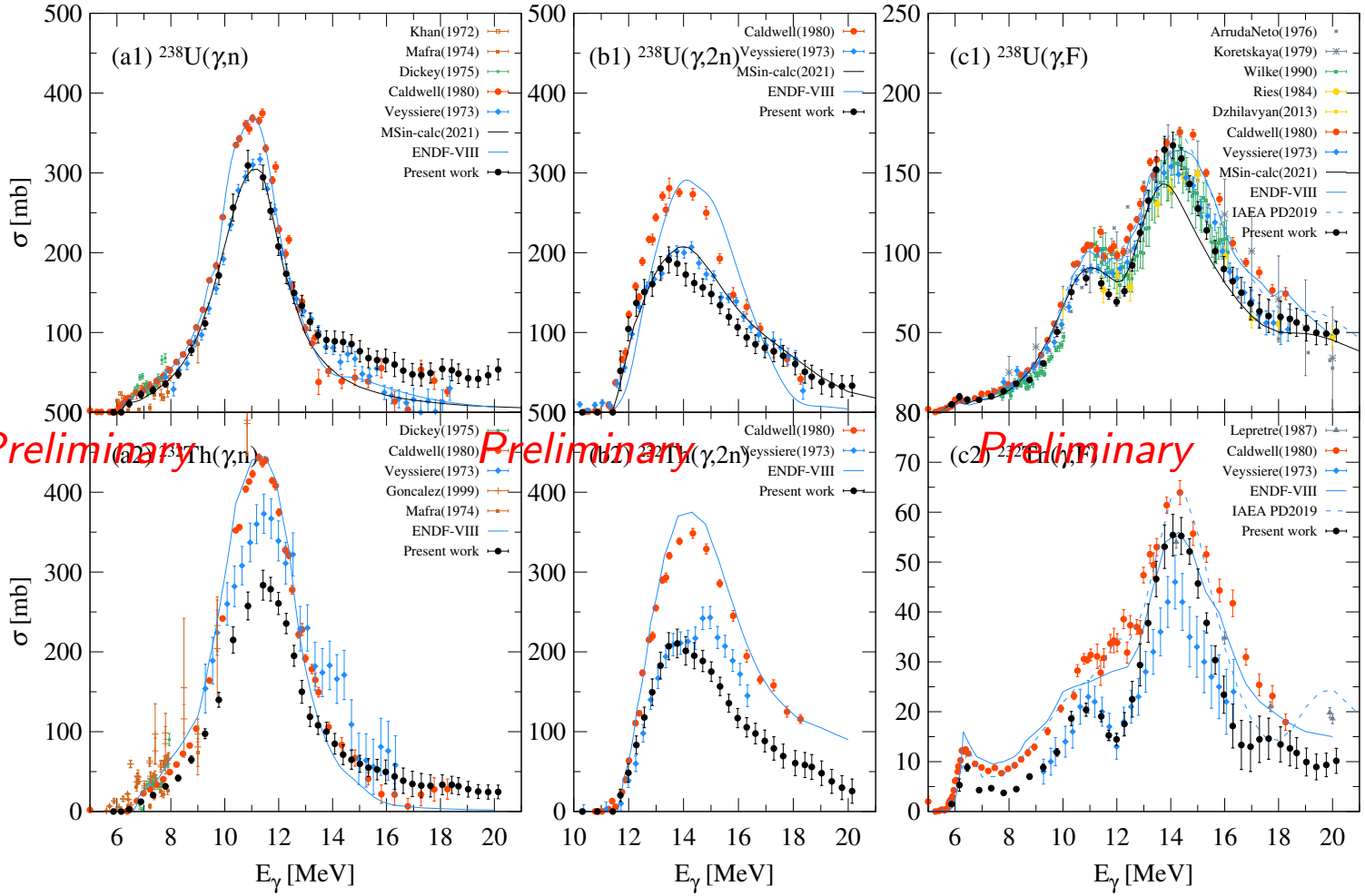

Present results (black dots) and existing data obtained with positron in flight annihilation beams at Saclay (blue full diamonds), Livermore (red full dots), Giessen (yellow full dots) and Moscow (yellow full square), bremsstrahlung beams (gray), bremsstrahlung monochromators (green), capture γ-rays (brown).

Preliminary results - ^{238}U and ^{232}Th photoabsorption cross sections

$$\sigma_{\gamma,\,abs} = \sigma_{\gamma,\,n} + \sigma_{\gamma,\,2n} + \sigma_{\gamma,\,3n} + \sigma_{\gamma,\,F}$$

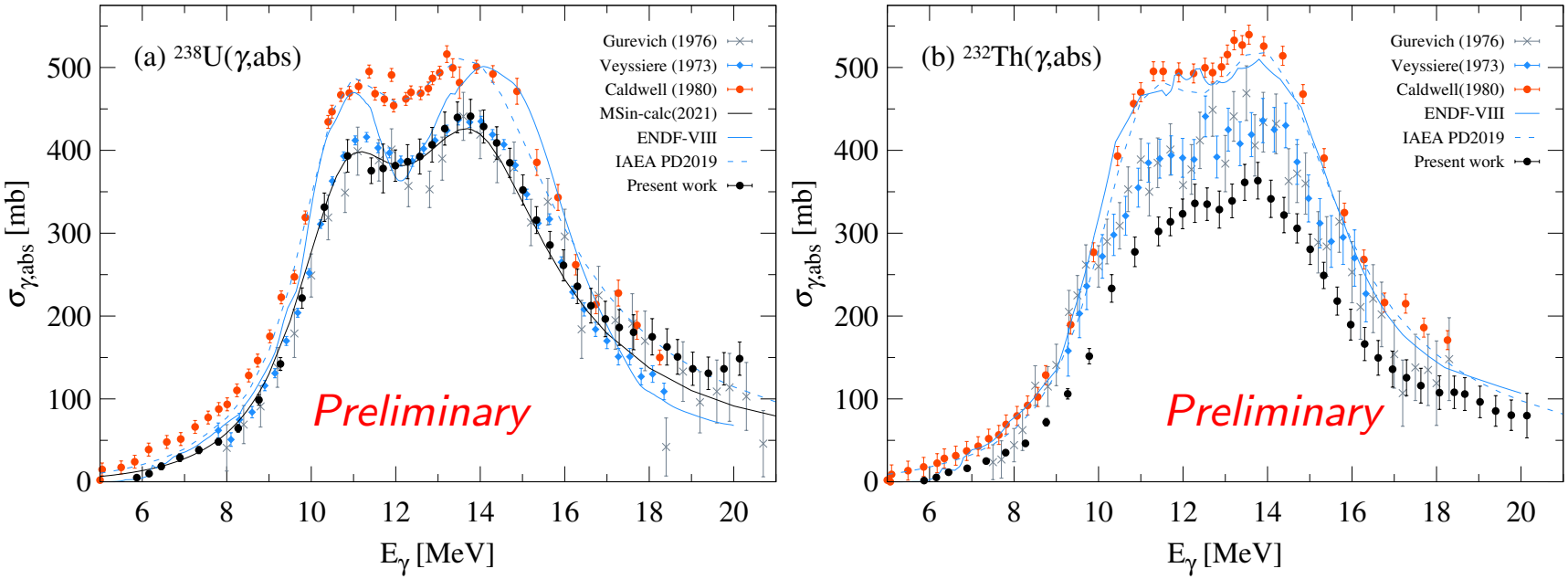

Present photon absorbtion cross sections for (a) ^{238}U and (b) ^{232}Th compared with existing data obtained with positron in flight annihilation beams at Saclay - Veyssiere NPA **199**, 45 (1973) (blue full diamonds) and at Livermore - Caldwell PRC **21**, 1215 (1980) (red full dots), with bremsstrahlung beams (gray) and also with recent statistical model calculations ▸ M.Sin PRC 103, 054605 (2021)

Preliminary results - ^{238}U and ^{232}Th low energy photofission cross sections

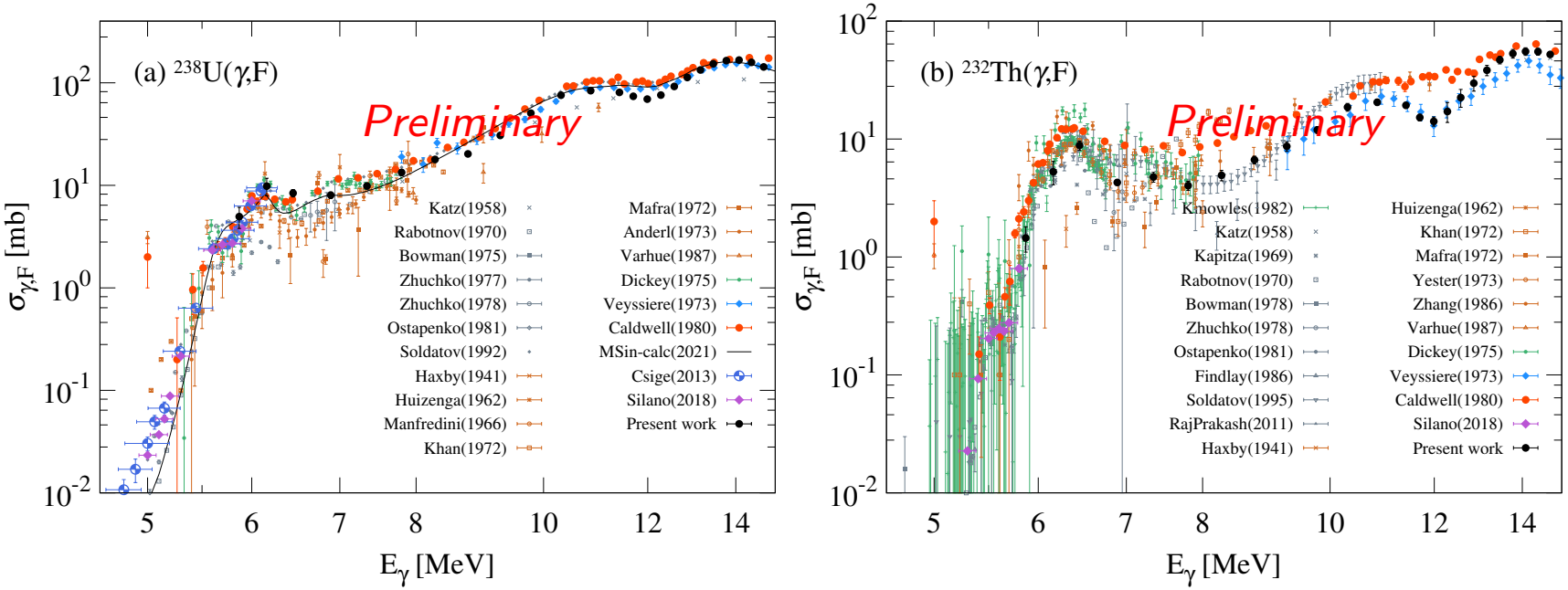

Present $\sigma_{\gamma,F}$ (black full dots) and existing data in the low energy region: recent LCS γ-ray beam data obtained at HIγS by ▸ Csige (PhysRevC.87.044321) (blue half-empty dots) using a fission chamber and by ▸ Silano (PhysRevC.98.054609) (purple full diamonds) using a moderated ^{3}He detection array, the Saclay (blue full diamonds) and Livermore (red full dots) positron in flight annihilation data, bremsstrahlung data (gray symbols), bremsstrahlung monocromator data (green symbols), capture γ-ray data (brown symbols).

Preliminary results - ^{238}U and ^{232}Th average energies of PFNs

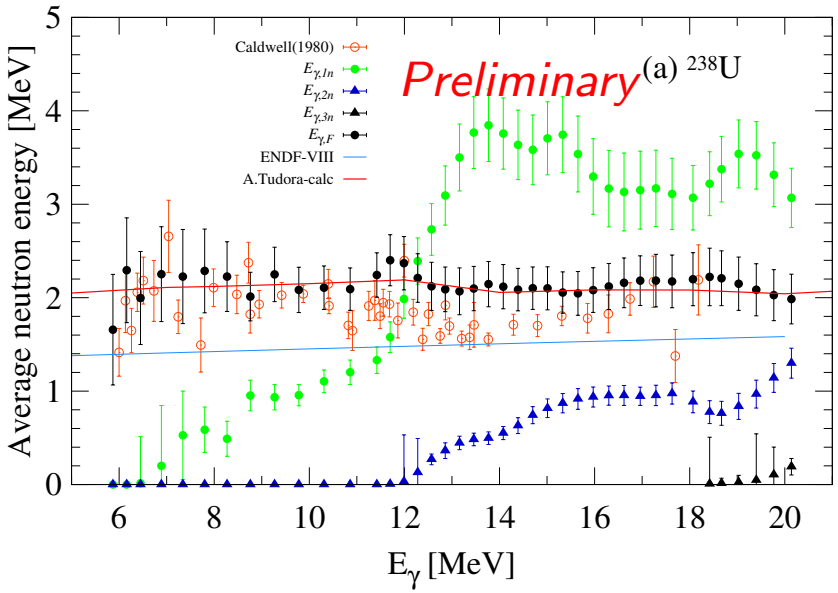

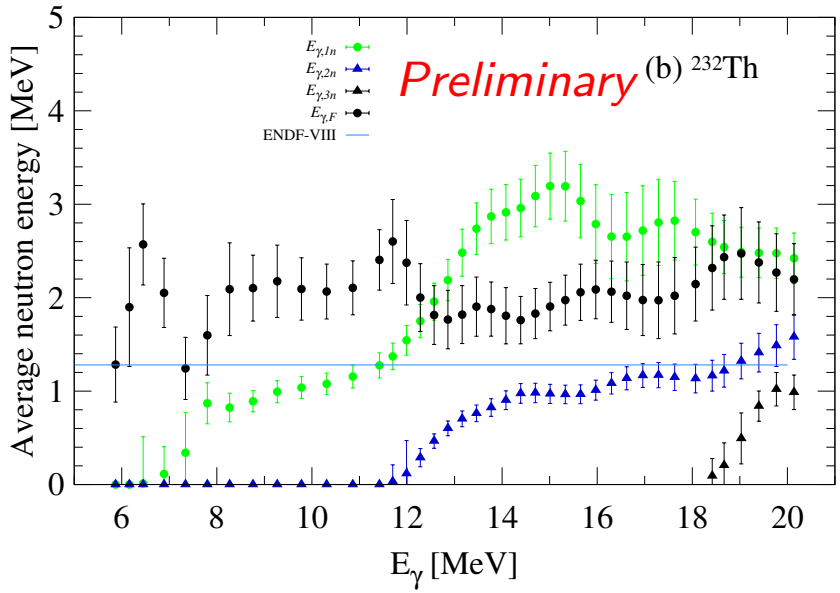

Preliminary results - ^{238}U and ^{232}Th mean PFN multiplicities

Dependence with incident photon energy for the mean PFN multiplicities in the photofission reactions on (a) ^{238}U and (b) ^{232}Th. The present results (full black dots) are compared with recent HIγS LCS γ-ray beam data of Silano (PhysRevC.98.054609) (purple full diamonds), Livermore positron in flight annihilation data (full red dots), capture γ-ray data (brown symbols) and bremsstrahlung data (gray open triangle). The blue solid lines show the systematic linear dependences deduced from neutron-induced fission experiments by Soleilhac et al. and used by the Saclay group in the data reduction. The full black lines are predictions obtained through calculations in the frame of the most probable fragmentation approach with the Los Alamos model.

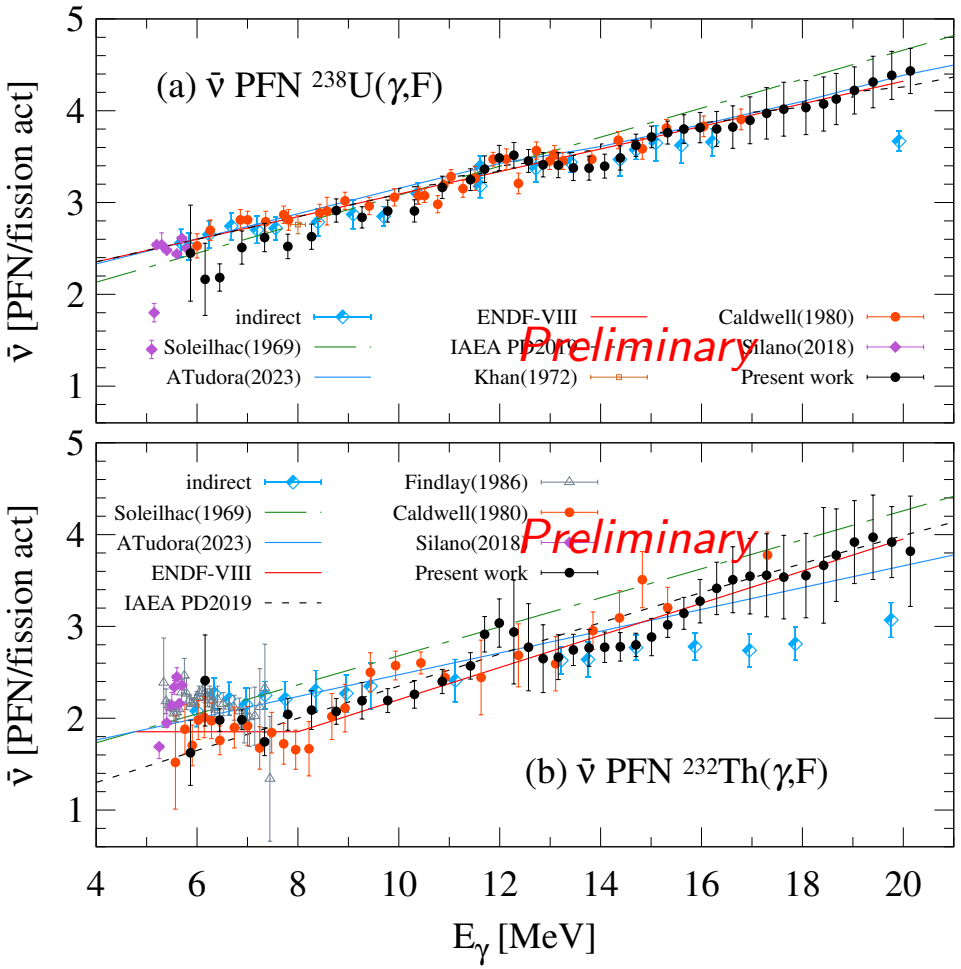

Summary on ^{238}U and ^{232}Th photoneutron and photofission data

Results:

- Photoneutron and photofission investigations in the $\sim S_n$ up to 20 MeV using LCS γ-ray beams.
- Neutron multiplicities recorded with with moderated ^{3}He neutron detection array of $\sim$37% energy independent efficiency.
- Neutron multiplicity sorting:
  - photoneutron and photofission discrimination based on modelling the PFNs multiplicity with a Gaussian;
  - corrected for *multiple-firings* efects
- Measured:
  - photoneutron cross sections and average energies;
  - photofission cross sections, PFNs average energies and mean numbers of PFNs per fission act;

Future work:

- Separate the fission cross section into its first and second chance components, based on the PFN energies.
- Statistical model calculations.